

Collard, L. R. B. Elton, and R. Hofstadter, in *Landolt-Bornstein Numerical Data and Functional Relationships in Science and Technology*, edited by K.-H. Hellwege

and H. Schopper (Springer-Verlag, Berlin, Germany, 1967), New Series, Group I, Vol. 2.

<sup>18</sup>P. Federman and S. Pittel, to be published.

PHYSICAL REVIEW C

VOLUME 2, NUMBER 6

DECEMBER 1970

## Energy Levels in <sup>86</sup>Sr from the Decay of 14.6-h <sup>86</sup>Y

A. V. Ramayya, B. Van Nooijen,\* J. W. Ford, D. Krmpotić,† and J. H. Hamilton  
*Physics Department, ‡ Vanderbilt University, Nashville, Tennessee 37203*

and

J. J. Pinajian and Noah R. Johnson  
*Oak Ridge National Laboratory, § Oak Ridge, Tennessee 37803*  
 (Received 20 April 1970)

The radioactive decay of <sup>86</sup>Y has been investigated by performing internal- and external-conversion measurements with an iron-free double-focusing  $\beta$ -ray spectrometer,  $\gamma$ -ray measurements with Ge(Li) spectrometers, and  $\gamma$ - $\gamma$  coincidence experiments with NaI-NaI, NaI-Ge(Li), and Ge(Li)-Ge(Li) coincidence arrangements coupled to two-parameter analyzers. Coincidence relationships were used extensively to aid in the construction of a level scheme for <sup>86</sup>Sr. Excited states are established at 1076.63, 1854.20, 2229.68, 2481.91, 2642.27, 2672.76, 2788.2, 2878.28, 2997.34, 3055.66, 3185.19, 3291.08, 3317.58, 3362.06, 3499.84, 3555.71, 3644.94, 3686.74, 3765.59, 3774.80, 3831.06, 3871.53, 3925.89, 3942.41, 3968.84, 4146.0, 4206.00, 4339, 4410.5, 4718, and 4954 keV. The *K* conversion coefficient was directly measured for the 1076.63-keV transition and this transition was used to obtain *K* conversion coefficients from the relative  $\gamma$ -ray intensities and the relative conversion-electron intensities. A new decay scheme is proposed which removes the inconsistencies of the older scheme and gives a much more detailed picture of the decay properties of the <sup>86</sup>Y nucleus.

### I. INTRODUCTION

In recent years there has been considerable interest in the collective properties of spherical even-even nuclei. Numerous models have been used in an attempt to explain the low-lying levels in these nuclei. The most successful of these probably has been the vibrational model, and within this framework, particular interest has centered around the  $0^+$ ,  $2^+$ , and  $4^+$  members of the two-phonon triplet. The Bohr-Mottelson concept<sup>1</sup> of collective quadrupole motion of many nucleons appears to be applicable to the low-lying levels of many of these nuclei. The decay of <sup>86</sup>Y to <sup>86</sup>Sr has large decay energy and is thus well suited to study the energy levels to relatively high energy for comparison with theory. Single-particle calculations have also been carried out by Talmi and Unna<sup>2</sup> for the <sup>86</sup>Sr levels.

The decay of <sup>86</sup>Y (14.6 h), which has  $4^-$  ground-state spin-parity, to the levels of <sup>86</sup>Sr has been studied previously by Yamazaki, Ikegami, and Sakai<sup>3</sup> and Van Nooijen *et al.*<sup>4</sup> The level scheme proposed in Ref. 4 is shown in Fig. 1. The decay schemes proposed by both the groups differed very considerably. It was pointed out<sup>4</sup> that the decay

scheme proposed in their paper was not quite consistent, since it presented some difficulties with regard to intensities and multipolarities of certain transitions (for example, the 628- and 646-keV  $\gamma$  rays). The indications were that part of the internal-conversion and/or  $\gamma$ -ray intensities might be wrong, and further, that some transitions might have been missed. Thus far the  $\gamma$ -ray spectrum from the decay of <sup>86</sup>Y has been studied only with NaI detectors. To remove some of the uncertainties from the decay scheme, and thus make a better comparison with available nuclear models possible, we have studied in detail the conversion-electron spectrum with an iron-free double-focusing spectrometer, and the  $\gamma$ -ray singles and  $\gamma$ - $\gamma$  coincidence spectra with high-resolution Ge(Li) detectors and three-dimensional analyzer systems.

### II. SOURCE PREPARATIONS

The <sup>86</sup>Y activity was prepared in the Oak Ridge National Laboratory 86-in. cyclotron by the <sup>86</sup>Sr- $(p, n)$ <sup>86</sup>Y reaction. The beam energy was degraded to 12 MeV by the use of aluminum absorbers to reduce the production of 14-h <sup>87m</sup>Y and 80-h <sup>87</sup>Y from <sup>88</sup>Sr. The targets consisted of 100-mg samples of

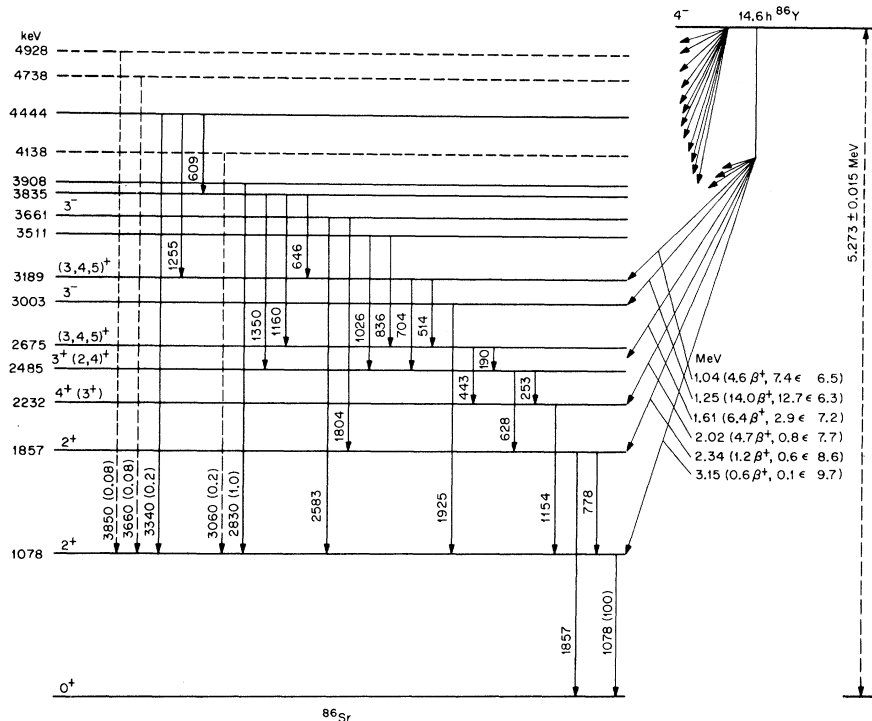


FIG. 1. The decay scheme of  $^{86}\text{Y}$  proposed by Van Nooijen *et al.* (Ref. 4).

97.6% isotopically enriched  $^{86}\text{Sr}$  as  $\text{SrCO}_3$  and were wrapped in 0.001-in. nickel foil. A beam current of 80  $\mu\text{A}$  was employed. The yield of  $^{86}\text{Y}$  was 10.5 mCi/h. Approximately 0.96% (10  $\mu\text{Ci}$ ) of  $^{88}\text{Y}$  as well as negligible quantities of  $^{87}\text{Y}$  were produced concomitantly.

Following irradiation, the nickel target was dissolved in 12  $M$   $\text{HCl}$  with the aid of 30%  $\text{H}_2\text{O}_2$ . The yttrium activity was isolated by radiocolloidal precipitation with 14.8  $M$   $\text{NH}_4\text{OH}$ . The small amount of iron normally found in the nickel foil helped scavenge the activity. The  $\text{Fe}(\text{OH})_3$  precipitate with the adsorbed  $^{86}\text{Y}$  was isolated by filtration, washed with dilute ammonium hydroxide, and dissolved in a minimum amount of 9  $M$   $\text{HCl}$ . The radiocolloidal precipitation was repeated, and the 9  $M$   $\text{HCl}$  solution was passed through a Bio-Rad AG-1 50–100-mesh anion-exchange resin (previously equilibrated with 9  $M$   $\text{HCl}$ ). The  $^{86}\text{Y}$  passed through the column, while iron and the  $^{57}\text{Co}$  contaminants were retained on the resin. One column volume rinse with 9  $M$   $\text{HCl}$  sufficed to wash off the remaining  $^{86}\text{Y}$  activity. The eluate was carefully evaporated down to dryness, treated three times with 15.7  $M$   $\text{HNO}_3$  to destroy organic material, and then treated with 12  $M$   $\text{HCl}$  to convert the product to the chloride. The activity was taken up in 0.1  $M$   $\text{HCl}$  and was essentially solids free and radiochemically pure.

### III. $\gamma$ -RAY ENERGY AND INTENSITY MEASUREMENTS

The  $\gamma$ -ray singles spectrum was studied by means of 2-, 6-, and 35-cm<sup>3</sup>  $\text{Ge}(\text{Li})$  detectors. The spectra, obtained with 2- and 6-cm<sup>3</sup> detectors were used mainly to distinguish escape peaks from full-energy peaks. The  $\gamma$ -ray spectrum measured with the 35-cm<sup>3</sup>  $\text{Ge}(\text{Li})$  detector was used to calculate the energies and relative intensities of the  $\gamma$  rays. In this case the detector was coupled to a Tennelec TC-135 preamplifier, a TC-207 main amplifier, and a Nuclear Data 4096-channel analyzer. The resolution of the system was 2.8 keV for the 1332.5-keV line of  $^{60}\text{Co}$ . The efficiency of the detector was 3.5% of that of a 3.0-in.  $\times$  3.0-in.  $\text{NaI}(\text{Tl})$  detector. The singles spectrum up to 1785 keV is shown in Fig. 2.

Separate measurements of the high-energy region of the  $\gamma$  spectrum were made with a 30-cm<sup>3</sup> detector coupled to a 1024-channel analyzer via a TC-135 preamplifier, a TC-200 main amplifier, and a TC-250 post-biased amplifier. This system had a resolution of 3.5 keV for the 1332.5-keV line of  $^{60}\text{Co}$ . The high-energy portion of the  $\gamma$  spectrum is shown in Fig. 3.

In all runs, 2.00 g/cm<sup>2</sup> of polystyrene was inserted between the source and detector to absorb



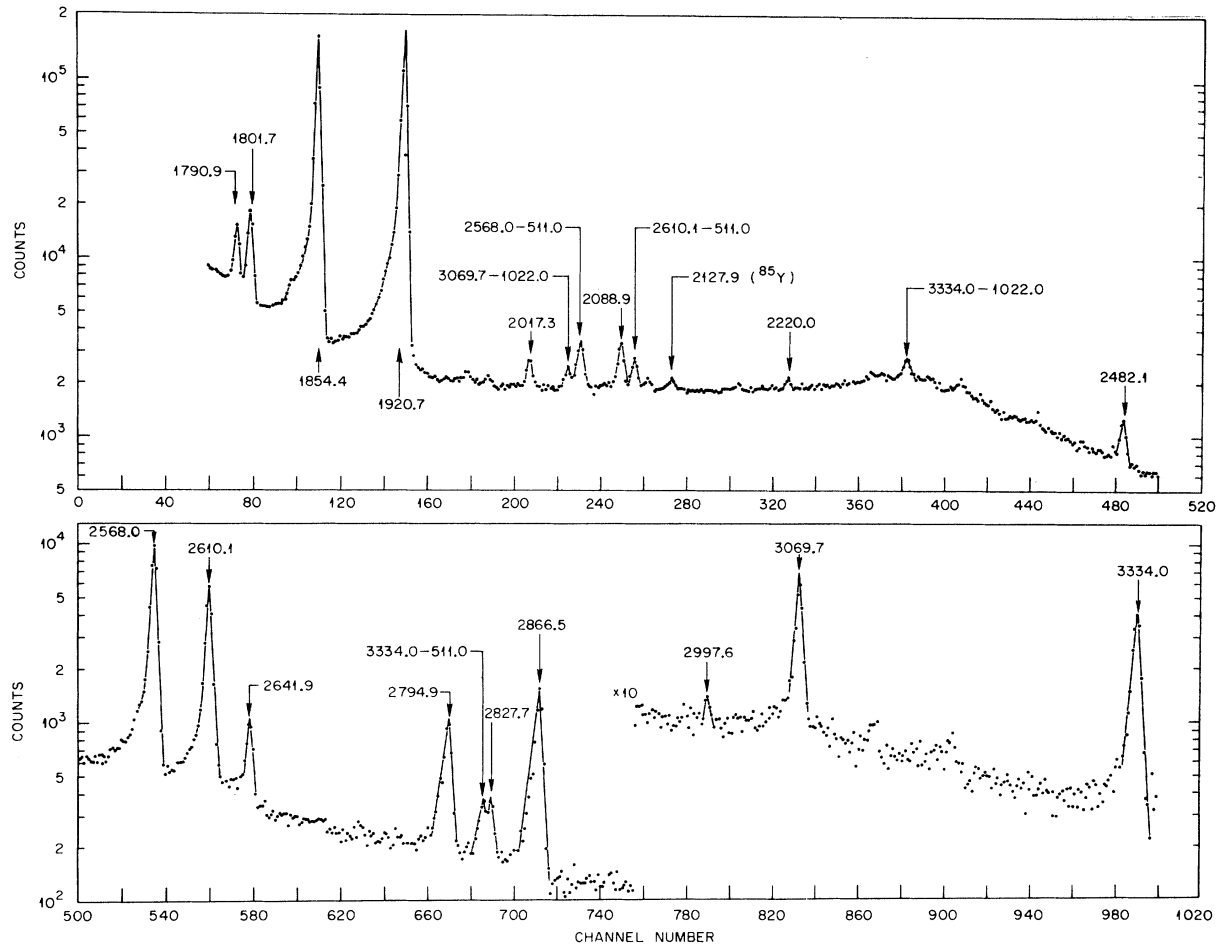


FIG. 3.  $\gamma$ -ray spectrum of  $^{86}\text{Y}$  in the energy region 1700–3500 keV.

longer time periods. The energies, in keV, used for the standard lines were:  $121.97 \pm 0.05$  ( $^{57}\text{Co}$ ),  $136.33 \pm 0.04$  ( $^{57}\text{Co}$ ),  $238.61 \pm 0.023$  ( $^{228}\text{Th}$ ),  $279.17 \pm 0.02$  ( $^{203}\text{Hg}$ ),  $320.10 \pm 0.03$  ( $^{51}\text{Cr}$ ),  $511.006 \pm 0.002$  ( $^{22}\text{Na}$ ),  $583.138 \pm 0.023$  ( $^{228}\text{Th}$ ),  $661.615 \pm 0.030$  ( $^{137}\text{Cs}$ ),  $897.98 \pm 0.05$  ( $^{88}\text{Y}$ ),  $1173.22 \pm 0.03$  ( $^{60}\text{Co}$ ),  $1332.505 \pm 0.025$  ( $^{60}\text{Co}$ ),  $1592.47 \pm 0.10$  (double escape of  $^{208}\text{Tl}$ ),  $1836.10 \pm 0.05$  ( $^{88}\text{Y}$ ),  $2103.46 \pm 0.10$  (single escape of  $^{208}\text{Tl}$ ), and  $2614.47 \pm 0.10$  ( $^{208}\text{Tl}$ ). The energy calibration was accomplished by a computer least-squares fit of the standard lines to a third-degree polynomial. The constants thus obtained were used to calculate the energies of the  $\gamma$  rays in the decay of  $^{86}\text{Y}$ . The efficiency calibration of the spectrometer was accomplished with the standard sources obtained from the International Atomic Energy Agency of Vienna, Austria. The results of the analysis of the spectra are summarized in Table I.

Although present in very minute quantities, the following contaminations of the  $^{86}\text{Y}$  sources were

identified: 14-h  $^{87}\text{Y}$  (381.8 keV), 80-h  $^{87m}\text{Y}$  (387.5 and 484.6 keV), and 105-day  $^{88}\text{Y}$  (897.9 and 1836.1 keV).

#### IV. INTERNAL-CONVERSION MEASUREMENTS

Internal-conversion experiments were carried out in the Vanderbilt iron-free double-focusing  $\beta$  spectrometer.<sup>6</sup> A Geiger-Müller counter was used as a detector; the cutoff of its window was about 10 keV.

Carrier-free sources were made on Zapon films by the liquid-drop method. The films were rendered conductive by evaporating approximately 8- $\mu\text{g}/\text{cm}^2$  aluminum onto them. Four sources have been used. Three of them (sources 1, 2, and 4) had areas of 5 mm  $\times$  16 mm; the relative half width of the conversion lines was about 0.5%. Source 3 had an area of 1.5 mm  $\times$  16 mm only, and the resolution obtained with this source was about 0.2%.

Some of the more interesting parts of the internal-conversion spectrum are shown in Figs. 4–7.

TABLE I. Energies and intensities of  $\gamma$  rays in  $^{86}\text{Sr}$  from the decay of  $^{86}\text{Y}$ .

Transition energy (keV)	Relative intensity	Transition energy (keV)	Relative intensity
132.34 $\pm$ 0.10	0.20 $\pm$ 0.01	1024.04 $\pm$ 0.10	4.6 $\pm$ 0.2
144.5 $\pm$ 0.3	0.038 $\pm$ 0.004	1076.63 $\pm$ 0.10	100
182.34 $\pm$ 0.20 <sup>a</sup>	0.13 $\pm$ 0.04	1087.6 $\pm$ 0.5	0.05 $\pm$ 0.01
187.87 $\pm$ 0.13	1.53 $\pm$ 0.05	1092.68 $\pm$ 0.13	0.84 $\pm$ 0.05
190.80 $\pm$ 0.13	1.23 $\pm$ 0.04	1102.02 $\pm$ 0.23	0.24 $\pm$ 0.03
209.80 $\pm$ 0.23 <sup>a</sup>	0.48 $\pm$ 0.02	1133.3 $\pm$ 1.0	0.36 $\pm$ 0.03
235.37 $\pm$ 0.23	0.48 $\pm$ 0.02	1142.3 $\pm$ 1.0 <sup>a</sup>	0.12 $\pm$ 0.04
237.9 $\pm$ 0.3	0.16 $\pm$ 0.03	1150.34 $\pm$ 0.18 <sup>c</sup>	very weak
252.05 $\pm$ 0.13	0.45 $\pm$ 0.02	1153.05 $\pm$ 0.10	37.0 $\pm$ 1.1
256.38 $\pm$ 0.4 <sup>a</sup>	0.09 $\pm$ 0.03	1154 $\pm$ 1.5	very weak
264.53 $\pm$ 0.13	0.65 $\pm$ 0.03	1163.03 $\pm$ 0.10	1.43 $\pm$ 0.05
307.00 $\pm$ 0.10	4.2 $\pm$ 0.1	1253.11 $\pm$ 0.10	1.86 $\pm$ 0.06
331.08 $\pm$ 0.23	1.01 $\pm$ 0.03	1270.16 $\pm$ 0.13	0.79 $\pm$ 0.12
355.07 $\pm$ 0.26	0.12 $\pm$ 0.03	1283.96 $\pm$ 0.13	0.35 $\pm$ 0.13
370.28 $\pm$ 0.17	1.00 $\pm$ 0.05	1294.9 $\pm$ 0.3	0.35 $\pm$ 0.10
380.4 $\pm$ 0.3	0.55 $\pm$ 0.04	1296.03 $\pm$ 0.23	0.66 $\pm$ 0.04
382.86 $\pm$ 0.23	4.40 $\pm$ 0.14	1327.5 $\pm$ 0.5	0.11 $\pm$ 0.05
425.97 $\pm$ 0.23	0.37 $\pm$ 0.02	1349.15 $\pm$ 0.10	3.57 $\pm$ 0.11
439.5 $\pm$ 0.3	0.24 $\pm$ 0.08	1404.8 $\pm$ 0.4	0.22 $\pm$ 0.06
443.13 $\pm$ 0.10	20.48 $\pm$ 0.59	1415.20 $\pm$ 0.23	0.40 $\pm$ 0.11
444.18 $\pm$ 0.23	0.78 $\pm$ 0.20 <sup>b</sup>	1507.86 $\pm$ 0.10	0.43 $\pm$ 0.05
448.10 $\pm$ 0.02 <sup>a</sup>	0.09 $\pm$ 0.03	1533.19 $\pm$ 0.13	0.27 $\pm$ 0.04
469.24 $\pm$ 0.25	0.36 $\pm$ 0.03	1535.67 $\pm$ 0.13	0.14 $\pm$ 0.04
503.0 $\pm$ 0.4	0.11 $\pm$ 0.04	1564.4 $\pm$ 0.5 <sup>a</sup>	0.22 $\pm$ 0.06
512.42 $\pm$ 0.16 <sup>c</sup>	very weak	1696.25 $\pm$ 0.13	0.77 $\pm$ 0.02
515.18 $\pm$ 0.20	5.93 $\pm$ 0.17	1711.6 $\pm$ 0.7	0.21 $\pm$ 0.04
580.57 $\pm$ 0.10	5.80 $\pm$ 0.17	1724.15 $\pm$ 0.10	0.67 $\pm$ 0.05
608.29 $\pm$ 0.10	2.44 $\pm$ 0.18	1790.90 $\pm$ 0.10	1.21 $\pm$ 0.05
618.24 $\pm$ 0.40	0.26 $\pm$ 0.04	1801.70 $\pm$ 0.10	2.00 $\pm$ 0.06
627.72 $\pm$ 0.10	39.5 $\pm$ 1.2	1854.38 $\pm$ 0.13	20.8 $\pm$ 0.6
634.78 $\pm$ 0.02 <sup>a</sup>	0.11 $\pm$ 0.03	1920.72 $\pm$ 0.13	25.2 $\pm$ 0.8
644.82 $\pm$ 0.24 <sup>c</sup>	2.65 $\pm$ 0.40 <sup>b</sup>	1969.1 $\pm$ 0.7 <sup>d</sup>	0.06 $\pm$ 0.01
645.87 $\pm$ 0.17 <sup>c</sup>	11.1 $\pm$ 1.3 <sup>b</sup>	2017.1 $\pm$ 0.6	0.16 $\pm$ 0.02
648.6 $\pm$ 1.0	very weak	2088.09 $\pm$ 0.25	0.30 $\pm$ 0.03
689.29 $\pm$ 0.25	0.21 $\pm$ 0.04	2108.87 $\pm$ 0.33	0.06 $\pm$ 0.01
702.2 $\pm$ 0.6 <sup>d</sup>	0.3 $\pm$ 0.1	2180.8 $\pm$ 1.0	0.04 $\pm$ 0.01
703.33 $\pm$ 0.10	18.7 $\pm$ 0.5	2291.8 $\pm$ 0.5	0.15 $\pm$ 0.01
709.90 $\pm$ 0.10	3.18 $\pm$ 0.09	2482.08 $\pm$ 0.17	0.14 $\pm$ 0.01
719.17 $\pm$ 0.23	0.27 $\pm$ 0.04	2555.3 $\pm$ 1.7	0.033 $\pm$ 0.01
740.81 $\pm$ 0.13	1.65 $\pm$ 0.06	2567.97 $\pm$ 0.18	2.73 $\pm$ 0.13
767.63 $\pm$ 0.13	2.9 $\pm$ 0.4 <sup>b</sup>	2610.11 $\pm$ 0.20	1.50 $\pm$ 0.09
768.25 $\pm$ 0.16 <sup>c</sup>	0.39 $\pm$ 0.13 <sup>b</sup>	2641.9 $\pm$ 0.4	0.20 $\pm$ 0.05
777.37 $\pm$ 0.10	27.2 $\pm$ 0.7	2790.0 $\pm$ 1.0	0.013 $\pm$ 0.007
783.56 $\pm$ 0.26	0.32 $\pm$ 0.04	2794.9 $\pm$ 0.4	0.25 $\pm$ 0.02
826.02 $\pm$ 0.13	4.0 $\pm$ 0.1	2827.7 $\pm$ 0.8 <sup>d</sup>	0.07 $\pm$ 0.02
833.72 $\pm$ 0.18 <sup>c</sup>	1.8 $\pm$ 0.4 <sup>b</sup>	2862 $\pm$ 3	0.011 $\pm$ 0.005
835.67 $\pm$ 0.22 <sup>c</sup>	5.3 $\pm$ 0.7 <sup>b</sup>	2865.9 $\pm$ 0.3	0.46 $\pm$ 0.08
882.96 $\pm$ 0.17	0.3 $\pm$ 0.1	2997.6 $\pm$ 0.5	0.01 $\pm$ 0.005
887.40 $\pm$ 0.17	0.53 $\pm$ 0.05	3069.7 $\pm$ 0.4	0.14 $\pm$ 0.02
955.35 $\pm$ 0.20	1.26 $\pm$ 0.05	3334.0 $\pm$ 0.5	0.15 $\pm$ 0.02
971.43 $\pm$ 0.18	0.33 $\pm$ 0.04	3642 $\pm$ 2	0.05 $\pm$ 0.01
1017.93 $\pm$ 0.23	0.22 $\pm$ 0.14	3877 $\pm$ 6	0.06 $\pm$ 0.05

<sup>a</sup>Not conclusively shown to belong to  $^{86}\text{Sr}$ .<sup>b</sup>Obtained from coincidence analysis.<sup>c</sup>Deduced from energy levels.<sup>d</sup>Not placed in the decay scheme.

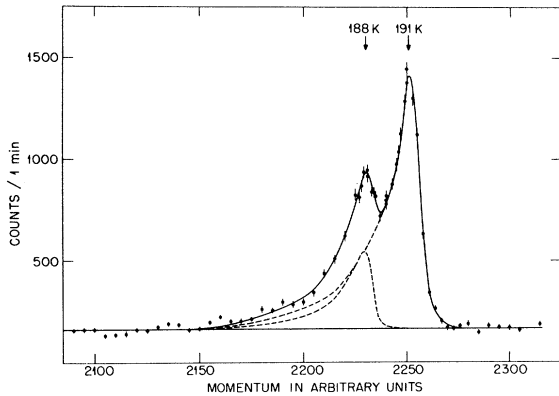


FIG. 4. Internal-conversion spectrum of the 188-191-keV doublet.

One notices that the 190-keV line is in fact a doublet consisting of 187.9- and 190.8-keV transitions; also, the 836-keV  $K$  conversion line is not pure but contains a contribution from the  $K$  conversion line of an 828.2-keV transition.

At a resolution of about 0.5%, the 628.1-keV  $L$  conversion line coincides with the 645.7-keV  $K$  conversion line; moreover, the 1160.0-keV  $K$  conversion peak cannot be separated properly from the 1153.8-keV  $K$  conversion line. Therefore, the 628.1-, 645.7-, 1077.9- (reference line), and 1153.8-keV  $K$  conversion lines, which are important for the decay scheme, were also measured with the spectrometer set at a resolution of 0.2%. These prolonged measurements were carried out with source 3.

Table II gives the results of the internal-conversion measurements. Column 1 lists the transition energies, and columns 2-5 present the intensities of the conversion lines relative to the intensity of the  $K$  conversion line of the 1077.9-keV transition. Part of the results described in Ref. 4 are given in column 6; the data of one particular run, which for unknown reasons are obviously wrong, have

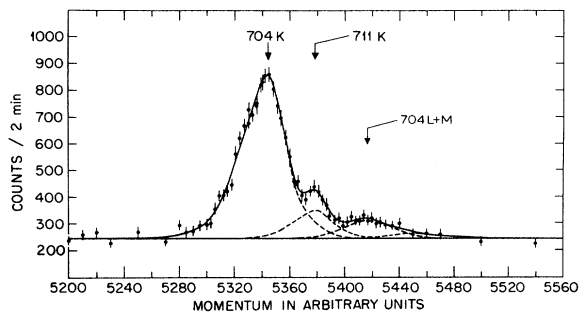


FIG. 5. Internal-conversion spectrum of the  $K$  lines of the 704- and 711-keV transitions. The highest-energy line is a composite of the  $L$  + higher-shell electrons from the 704-keV transition.

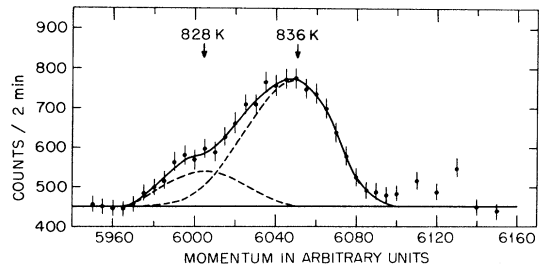


FIG. 6. Internal-conversion spectrum of the  $K$  lines of the 828- and 836-keV transitions.

been omitted. The relative conversion intensities mentioned in column 7 are the average values of those shown in columns 2-6.

#### V. INTERNAL-CONVERSION-COEFFICIENT MEASUREMENTS

The first internal-conversion-coefficient measurements were carried out by the internal-external-conversion (IEC) method. These data also provided more accurate values for the intensities of some important  $\gamma$  rays in our first work. After completion of some early measurements (1965), we decided to discontinue the external-conversion experiments, since more and better results with much less effort could be obtained employing Ge(Li) detectors which became available at about that time. In this section we present the few results which were obtained.

Sources 1, 2, and 3 mentioned in Sec. IV were also used in the external-conversion experiments. A 5-mm  $\times$  21-mm uranium converter, 3.78 mg/cm<sup>2</sup> thick, was placed in front of the source; the distance from source to converter was 0.19 cm. The external-conversion measurements were carried out in the double-focusing spectrometer under the same conditions as the internal-conversion experiments, the only difference being the presence of the uranium converter.

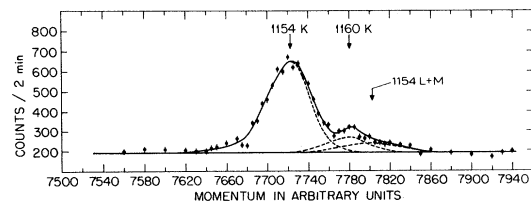


FIG. 7. Internal-conversion spectrum of the  $K$  lines of the 1154- and 1160-keV transitions. The highest-energy line is a composite of the  $L$  + higher-shell electrons from the 1154-keV transition. Evidence exists that there is a slightly larger tailing of the  $K$  line of the 1154-keV transition (on the higher-energy side) which would reduce the  $\alpha_K$  of the 1160-keV transition closer to the expected value.

TABLE II. Results of internal-conversion-electron measurements of transitions in  $^{86}\text{Sr}$  made with an iron-free double-focusing spectrometer.

Transition energy from electron data (keV)	Relative $K$ conversion intensity					Mean
	Source 1	Source 2	Source 3	Source 4	Ref. 4	
187.9 $\pm$ 0.5				73 $\pm$ 15		73 $\pm$ 15
190.8 $\pm$ 0.5				280 $\pm$ 20		280 $\pm$ 20
252.8 $\pm$ 0.5					4.2 $\pm$ 0.8	4.2 $\pm$ 0.8
307.1 $\pm$ 0.6				40 $\pm$ 4	38 $\pm$ 8	39.5 $\pm$ 3.5
331.6 $\pm$ 0.6				13 $\pm$ 4	19 $\pm$ 4	16 $\pm$ 3
442.9 $\pm$ 0.6	60 $\pm$ 7	62 $\pm$ 4				61.5 $\pm$ 3.5
513.5 $\pm$ 1.0	36 $\pm$ 7					36 $\pm$ 7
581.4 $\pm$ 1.0		18.0 $\pm$ 2.5				18.0 $\pm$ 2.5
609.0 $\pm$ 1.0		4 $\pm$ 1			4.6 $\pm$ 0.5	4.5 $\pm$ 0.5
628.1 $\pm$ 0.9	58 $\pm$ 4		53 $\pm$ 5			56 $\pm$ 3
645.7 $\pm$ 0.9	38.5 $\pm$ 4.5		37 $\pm$ 3			37.5 $\pm$ 2.5
704.1 $\pm$ 0.9	47 $\pm$ 4				42 $\pm$ 2	43 $\pm$ 2
710.8 $\pm$ 1.2	7 $\pm$ 3				8 $\pm$ 2	7.5 $\pm$ 2.0
777.8 $\pm$ 1.0	60 $\pm$ 6				55 $\pm$ 10	59 $\pm$ 5
828.2 $\pm$ 1.7		3 $\pm$ 1				3 $\pm$ 1
836.3 $\pm$ 1.1		11 $\pm$ 1			10 $\pm$ 1	10.5 $\pm$ 0.7
1025.6 $\pm$ 1.4		4 $\pm$ 1		6 $\pm$ 1	4.1 $\pm$ 0.4	4.4 $\pm$ 0.4
1077.9 $\pm$ 0.9	100	100	100	100	100	100
1153.8 $\pm$ 1.2	30 $\pm$ 3	33 $\pm$ 4	32 $\pm$ 3			32 $\pm$ 2
1160.0 $\pm$ 2.2	4.7 $\pm$ 2.5					4.7 $\pm$ 2.5
1255.0 $\pm$ 1.5					0.8 $\pm$ 0.2	0.8 $\pm$ 0.2
1350.3 $\pm$ 1.7					2.0 $\pm$ 0.3	2.0 $\pm$ 0.3
1804.3 $\pm$ 2.5					0.6 $\pm$ 0.2	0.6 $\pm$ 0.2
1856.7 $\pm$ 2.5					7.1 $\pm$ 1.1	7.1 $\pm$ 1.1
1924.3 $\pm$ 2.5					4.2 $\pm$ 0.8	4.2 $\pm$ 0.8

Internal-conversion coefficients can then be calculated<sup>7</sup> from these data on the internal- and external-conversion lines after the proper decay and momentum corrections are made. The results of these measurements are presented in Table III. The  $\alpha_K$  of the 1077.9-keV transition agrees well with the theoretical  $E2$  value<sup>8</sup> of  $4.32 \times 10^{-4}$ . A correction of about 9% has been applied to the intensity of the external  $K$  conversion line of the 628.1-keV transition to account for the contribution of the external  $M$  conversion line of the 511-keV annihilation quanta.

The  $K$  conversion coefficients of transitions in  $^{86}\text{Sr}$  have been calculated from the relative  $\gamma$ -ray intensities of Table I and the relative conversion-

electron intensities given in Table II. The theoretical  $E2$   $K$  conversion coefficient ( $4.32 \times 10^{-4}$ ) of the 1076.6-keV transition from the  $2^+$  first excited state to the  $0^+$  ground state was used as the standard to normalize the relative electron and  $\gamma$ -ray data. Table IV gives the conversion coefficients determined in this way in the present work. In Fig. 8, the experimental  $K$  conversion coefficients determined in this work are plotted against transition energy. The solid lines represent the theoretical values of  $K$  conversion coefficients<sup>8</sup> for  $E1$ ,  $E2$ , and  $M1$  transitions. For the 1163-keV transition the error is large because of uncertainties in analyzing the lines, but an  $E1$  multipolarity is definitely excluded. The conversion coefficients of the

TABLE III. Results of IEC  $K$  conversion coefficient measurements.

Transition energy from electron data (keV)	Internal $K$ conversion coefficient			Mean ( $\times 10^{-4}$ )
	Source 1 ( $\times 10^{-4}$ )	Source 2 ( $\times 10^{-4}$ )	Source 3 ( $\times 10^{-4}$ )	
628.1	6.3 $\pm$ 1.3	5.5 $\pm$ 1.3	5.6 $\pm$ 1.6	5.8 $\pm$ 0.8
777.8	11.4 $\pm$ 2.5	8.9 $\pm$ 2.5	9.9 $\pm$ 3.1	10.1 $\pm$ 1.6
1077.9	4.5 $\pm$ 0.5	3.7 $\pm$ 0.5	...	4.1 $\pm$ 0.4

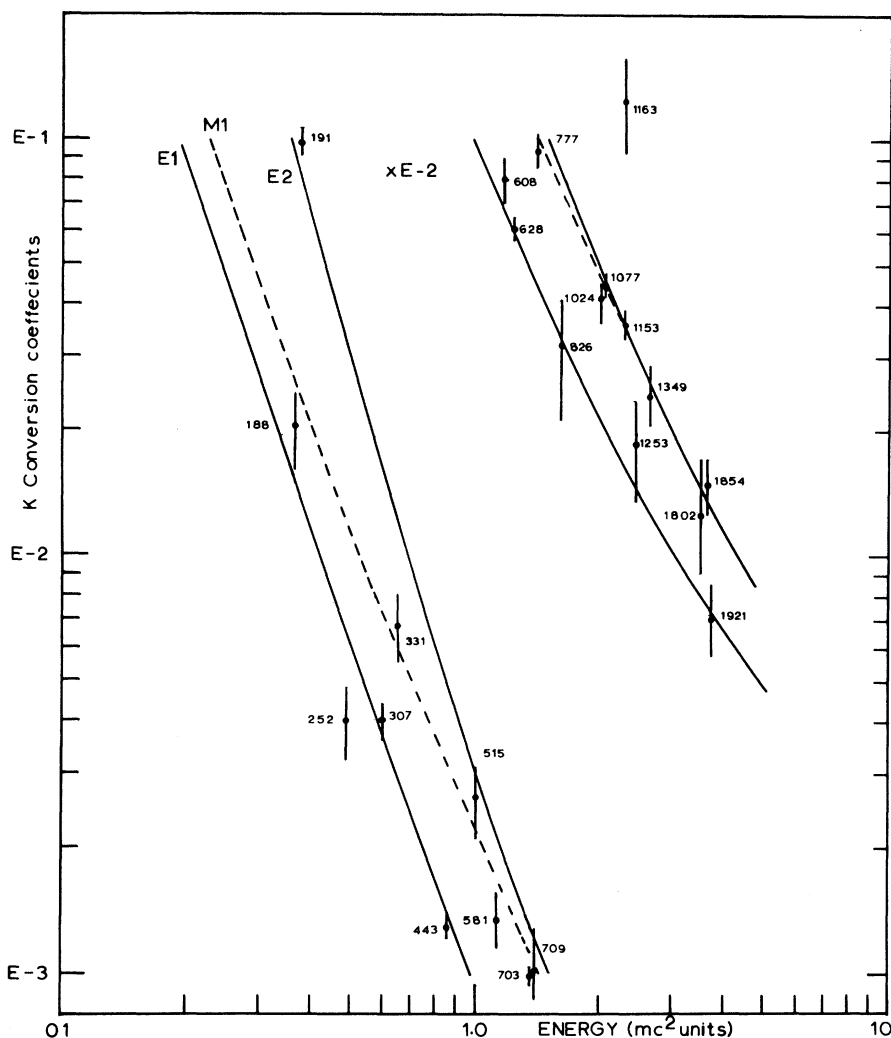


FIG. 8. Theoretical and experimental  $K$  conversion coefficients of transitions in  $^{86}\text{Sr}$  as a function of energy. The solid and dashed lines are the theoretical values of Hager and Seltzer (Ref. 8) for the identified multipoles.

628.1- and 777.8-keV transitions measured by the IEC method (see Table III) are in good agreement with the values listed in Table IV.

#### VI. $\gamma\text{-}\gamma$ COINCIDENCE EXPERIMENTS

$\gamma\text{-}\gamma$  coincidence measurements were performed with three different arrangements: (a) two 3.0-in.  $\times$  3.0-in. NaI(Tl) detectors coupled to a 100 by 200-channel analyzer, (b) a 3.0-in.  $\times$  3.0-in. NaI(Tl) detector and a 35-cm<sup>3</sup> Ge(Li) detector with a 4096 by 4096-channel Nuclear Data two-parameter analyzer, and (c) two 35-cm<sup>3</sup> Ge(Li) detectors coupled to a Nuclear Data 4096 by 4096-channel two-parameter analyzer.

The setup (a) consisted of two cylindrical NaI(Tl) 3.0-in.  $\times$  3.0-in. detectors coupled to an Oak Ridge

National Laboratory coincidence system set for 75-nsec resolving time. Coincidences and singles were recorded by a Victoreen (MP204RT) 100 by 200-channel multiparameter analyzer. The detectors were located at an angle of 90°, and a 3-cm-thick lead absorber was inserted between them to minimize crystal-to-crystal scattering.

Although most of the NaI-NaI and NaI-Ge(Li) coincidence measurements simply served to corroborate the later results obtained with two Ge(Li) detectors, the spectra coincident with 1076.6 keV are important in establishing which high-energy transition fed the first excited state, as discussed in Sec. VIII. The NaI-NaI (1076.6-keV gate) coincidence spectrum is shown in Fig. 9.

The remaining discussion of coincidence results will be for experiments performed with the Ge-Ge



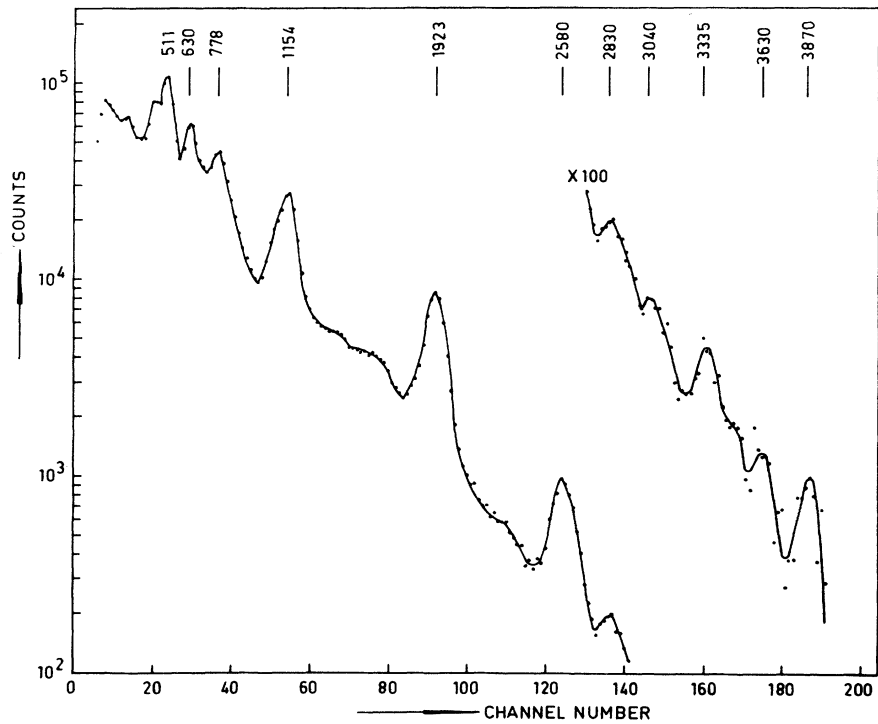


FIG. 9. Coincidence spectrum obtained with the gate set on the 1076.6-keV photopeak. The spectrum was obtained with a NaI-NaI system (a) (see text). The 2580- and 2830-keV peaks are a composite of 2567.97-, 2610.11-keV and 2794.90-, 2865.90-keV photopeaks, respectively. The weak peak at 3040 keV has an uncertainty of 30 keV. The other photopeaks in this region have uncertainties on the order of 15 keV.

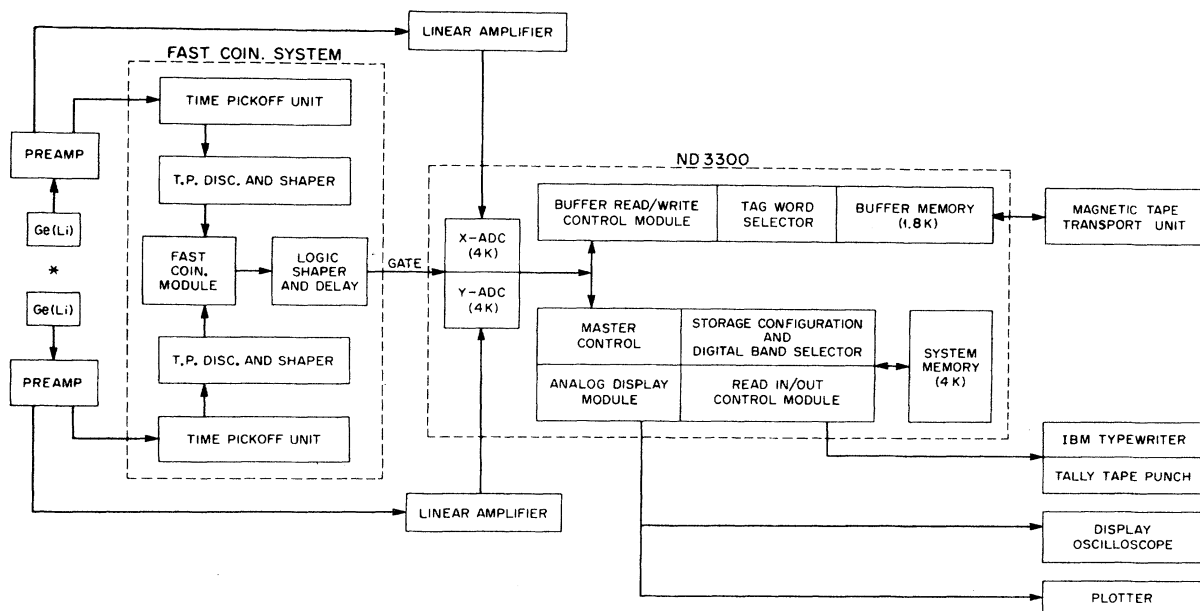


FIG. 10. Block diagram of the Vanderbilt Ge(Li)-Ge(Li) two-parameter coincidence system.

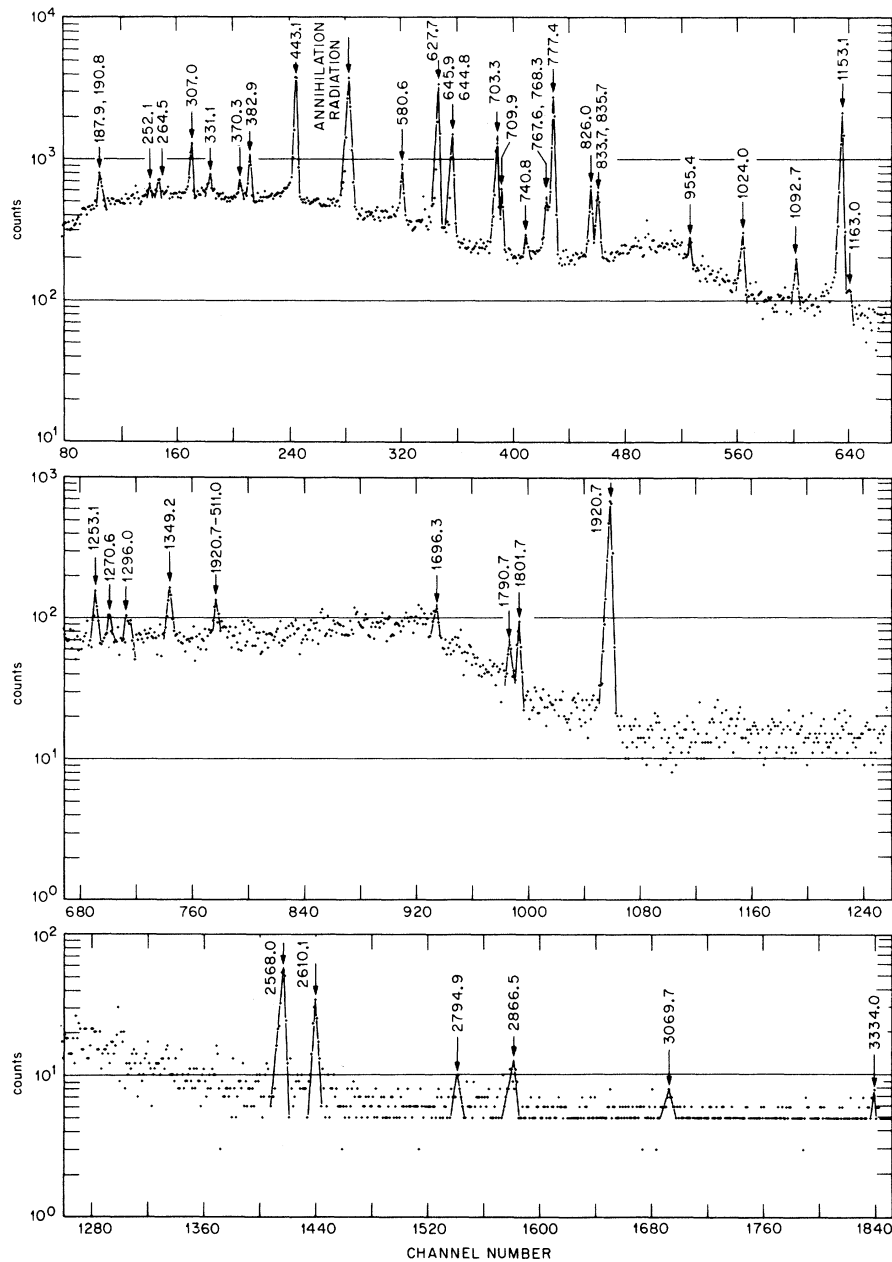


FIG. 11. Coincidence spectrum obtained from the 1076.6-keV gate taken with system (c) described in text. Although there is only weak evidence for the 2794.9-, 2865.9-, 3069.7-, and 3334.0-keV transitions in this spectrum, the first two of these were clearly seen in a Ge(Li)-NaI coincidence experiment (figure not shown) and the last two were evident in the NaI-NaI measurement (Fig. 9).

system. Measurements with this system superseded all others and with the one exception noted above give the most details of the decay properties. The two germanium detectors were located at  $90^\circ$  and were surrounded by lead cones to minimize crystal-to-crystal Compton scattering. An ORTEC fast-coincidence system ( $2\tau = 60$  nsec) with leading-edge timing was used to provide an external gate for a Nuclear Data two-dimensional

analyzer (ND 3300 system) equipped with a buffer memory and a magnetic-tape unit. The amplifier output from one of the Ge(Li) detectors was coupled to the Y analog-to-digital converter (ADC) and that from the other Ge(Li) detector to the X ADC. The total energy range covered in each dimension was 100 to 3500 keV. A block diagram of the system is shown in Fig. 10. The coincidence events were stored as elements of the type  $X_i Y_i$ ,

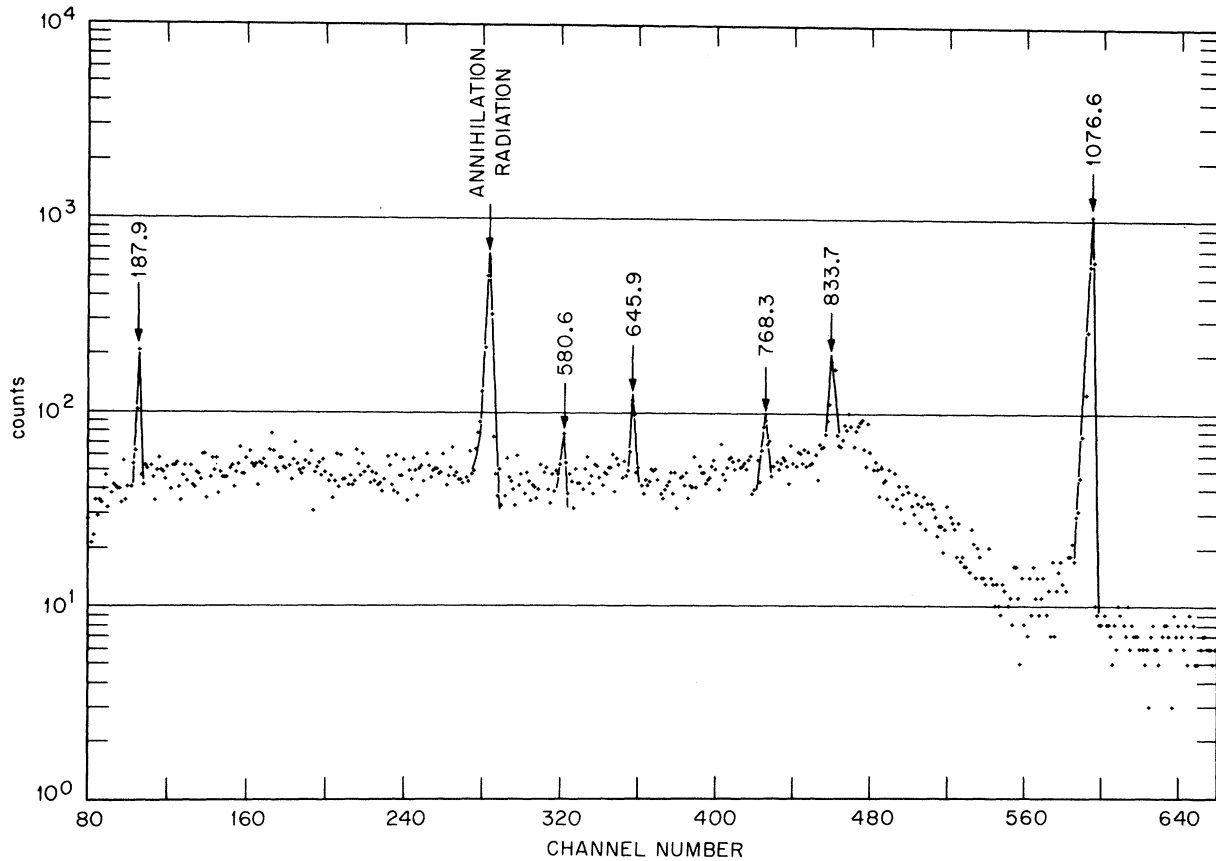


FIG. 12. Coincidence spectrum obtained with the gate set on the 1920.7-keV peak; taken with a Ge(Li)-Ge(Li) system (c) (see text).

on magnetic tape. Any  $Y_i$  spectrum could be recalled to the memory of the analyzer by specifying  $X_i$ . The spectrum of one of the detectors was stored in 2048 channels so that two 2048-channel coincidence spectra could be read into the analyzer memory simultaneously. Digital band-selector gates were set on the background, either above or just below the photopeaks, as well as on the photopeaks themselves, in order to correct for the Compton background coincidences. The source strength and resolving time were chosen such that chance coincidences could be neglected. This fact is convincingly demonstrated by the coincidence spectrum taken with the gate set on the photopeak of the 1076.6-keV  $\gamma$  ray; the 1076.6-keV chance coincidence peak is absent (see Fig. 11).

#### A. Coincidence Spectra and Analysis of Primary Cascades in $^{86}\text{Sr}$

Figures 11-23 are some of the coincidence spec-

tra which illustrate many of the important features of the decay scheme. Some of the less intense  $\gamma$  rays in these figures are not identified by energy in the figures but are included in the analysis. A summary of the coincidence relationships is given in Table V, and some of the important relationships are discussed in this section to provide the basis for the decay scheme discussion to follow. The entries in Table V reflect the strength of the peaks in the spectrum, compared with the strength of the peaks in the singles spectrum.

The positions of the 443.13-, 627.72-, 777.37-, 1076.63-, 1153.05-, 1854.38-, and 1920.72-keV  $\gamma$  rays in the  $^{86}\text{Sr}$  level scheme are well established.<sup>4</sup> The present coincidence experiments substantiate unequivocally the results of Van Nooijen *et al.*<sup>4</sup> rather than the other work.<sup>3</sup> The above-mentioned  $\gamma$  rays are placed in the decay scheme in the following way:

$$\begin{aligned}
 0 &\rightarrow (1076.63) \rightarrow 1076.63 \rightarrow (1920.72) \rightarrow 2997.34, \\
 0 &\rightarrow (1076.63) \rightarrow 1076.63 \rightarrow (777.37) \rightarrow 1854.20 \rightarrow (627.72) \rightarrow 2481.91, \\
 0 &\rightarrow (1076.63) \rightarrow 1076.63 \rightarrow (1153.05) \rightarrow 2229.68 \rightarrow (443.13) \rightarrow 2672.76.
 \end{aligned}$$

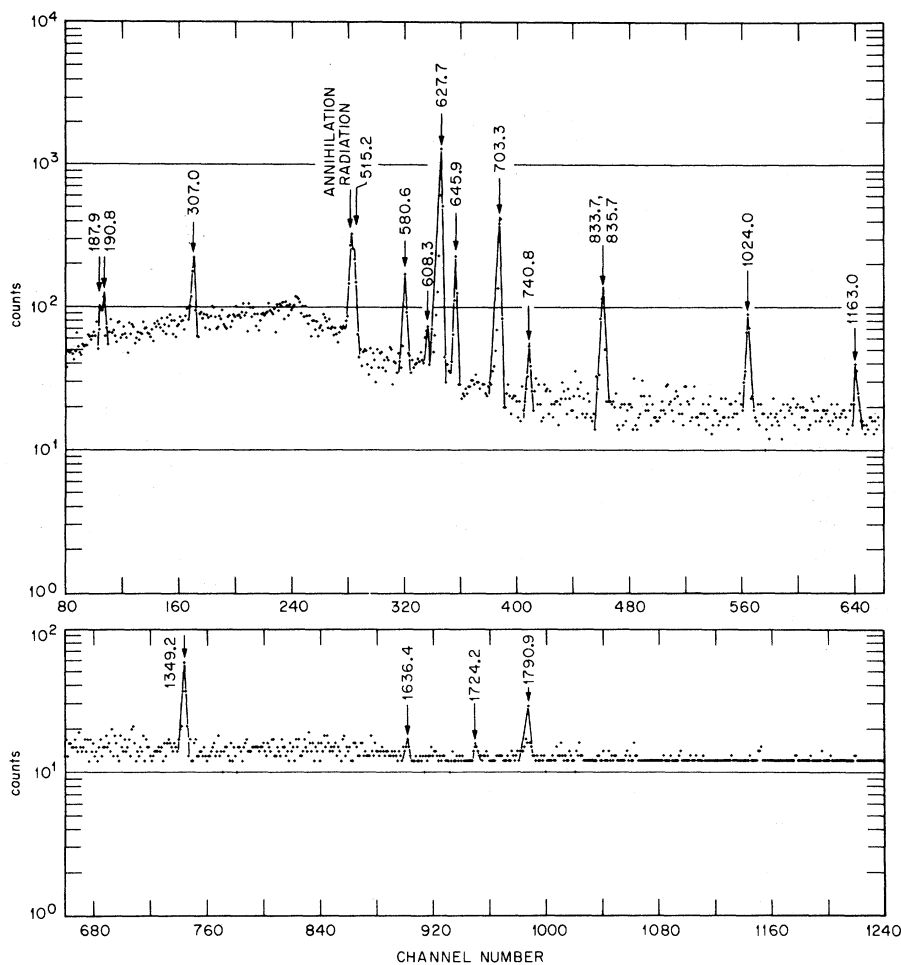


FIG. 13. Coincidence spectrum obtained with the gate set on the 1854.4-keV peak; taken with system (c) (see text).

The numbers in parentheses refer to the transition  $\gamma$  ray, in keV, which connects the levels indicated on either side, also in keV. The level energies quoted are the averages of the values obtained by different sums.

$$\text{B. } 0 \leftarrow (1076.63) \leftarrow 1076.63 \leftarrow (1920.72) \leftarrow 2997.34\text{-keV Cascade}$$

Figure 12 indicates that the 1920.72-keV  $\gamma$  ray is strongly in coincidence with the 1076.63-keV transition from the first excited  $2^+$  level to the ground-state  $0^+$  level. Figure 11 also shows that the 1920.72-keV  $\gamma$  ray is in coincidence with the 1076.63-keV line. In Fig. 12 we see in addition five clearly defined lines in coincidence with the 1920.72-keV  $\gamma$  ray. The presence of the sharp annihilation peak indicates that there is a substantial amount of  $\beta^+$  feeding to the level at  $1076.63 + 1920.72 = 2997.34$  keV. The sum of 645.9- and 187.9-keV  $\gamma$  rays suggests that the 833.7-keV  $\gamma$  ray is a crossover of these two transitions.

$$\text{C. } 0 \leftarrow (1076.63) \leftarrow 1076.63 \leftarrow (777.37) \leftarrow 1854.20 \leftarrow (627.72) \leftarrow 2481.91\text{-keV Cascade}$$

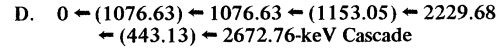
In Fig. 11 we see very clearly that the 1854.38-keV line is not in coincidence with the 1076.63-keV  $\gamma$  ray. This suggests that the 1854.38-keV  $\gamma$  ray is a transition to the ground state from the second excited  $2^+$  level. The intense 777.37-keV line is not in coincidence with the 1854.38-keV  $\gamma$  ray but is in coincidence with the 1076.63-keV line (see Fig. 11). This substantiates the placement of the 1854.38-keV  $\gamma$  ray as a crossover transition of the 1076.63- and 777.37-keV lines.

In the 1854-keV gate (see Fig. 13), the most intense line is the 627.72-keV one; and in the 627.7-keV gate, the 1854-keV line is the most intense one (see Fig. 14). These two spectra indicate that the 627.72-keV line directly feeds the 1854.20-keV level. The 703.33-keV  $\gamma$  ray is placed as feeding the  $1854.20 + 627.72 = 2481.91$ -keV level, since this line shows up strongly in the coincidence spectra taken with the 1854.38-, 1076.63-, and 627.72-keV

gates. Hence, a level is assigned at 2481.91 + 703.33 = 3185.19 keV. Similarly, the 1349.15-keV  $\gamma$  ray is placed as feeding the 2481.91-keV level to yield a level at 2481.91 + 1349.15 = 3831.06 keV.

When one enlarges the region of 511 keV in Fig. 14, the 515.18-keV  $\gamma$  ray clearly appears as a shoulder on the 511-keV annihilation radiation to establish that the 515.18-keV  $\gamma$  ray appears strongly in the spectrum gated on the 627.72-keV transition. The 515.18-keV transition does not appear in the 1920-keV gate. These facts substantiate the placement of this  $\gamma$  ray as the transition between the previously established 2997.34- and 2481.91-keV levels.

A relatively intense coincidence peak at 1724.15 keV was seen when the gate was set at 627.72 keV (see Fig. 14). This same transition appeared as a small peak in the coincidence spectra for gate settings of 1076.63 and 1854.38 keV (see Table V). Therefore a level is proposed at 2481.91 + 1724.15 = 4206.00 keV.



In the coincidence spectra obtained with the gate setting on the 1153.05-keV  $\gamma$  ray (see Fig. 15), the 1076.63-keV  $\gamma$  ray is observed very strongly, while in the gate at 1854.38 keV (see Fig. 13) the 1153.05-keV line is not observed. These data, coupled with the large intensity of the 1153.05-keV transition, restrict it to feed the 1076.63-keV first excited level. This cascade is further substantiated by the appearance of the 1153.05-keV transition very strongly in coincidence with the 1076.63-keV  $\gamma$  ray (see Fig. 11). These data establish a level at 1076.63 + 1153.05 = 2229.68 keV. The fact that the 1076.63- and 1153.05-keV transitions are by far the strongest transitions and are of equal intensity in the coincidence spectrum obtained by setting the window on the 443.13-keV  $\gamma$  ray restricts the 443.13-keV transition to feed the 2229.68-keV level to establish a 2672.76-keV level.

TABLE IV. Internal-conversion coefficients and multiplicities of transitions in  $^{86}\text{Sr}$ . The multipolarity assignments were made from comparison with Fig. 8.

Transition energy (keV)	Relative $\gamma$ -ray intensity	Relative K conversion-electron intensity	Internal-conversion coefficient ( $\alpha_K$ ) <sup>a</sup>	Multipolarity
187.87 $\pm$ 0.13	1.53 $\pm$ 0.040	73 $\pm$ 15	( 2.1 $\pm$ 0.4 ) $\times 10^{-2}$	E1 or M1
190.80 $\pm$ 0.13	1.23 $\pm$ 0.03	280 $\pm$ 20	( 9.8 $\pm$ 0.7 ) $\times 10^{-2}$	E2
252.05 $\pm$ 0.13	0.452 $\pm$ 0.018	4.2 $\pm$ 0.8	( 4.0 $\pm$ 0.8 ) $\times 10^{-3}$	E1
307.00 $\pm$ 0.10	4.23 $\pm$ 0.10	39.5 $\pm$ 3.5	( 4.0 $\pm$ 0.4 ) $\times 10^{-3}$	E1
331.08 $\pm$ 0.23	1.02 $\pm$ 0.03	16 $\pm$ 3	( 6.8 $\pm$ 1.3 ) $\times 10^{-3}$	M1/E2
443.13 $\pm$ 0.10	20.5 $\pm$ 0.6	61.5 $\pm$ 3.5	(12.9 $\pm$ 0.8 ) $\times 10^{-4}$	E1
515.18 $\pm$ 0.20	5.93 $\pm$ 0.17	36 $\pm$ 7	( 2.6 $\pm$ 0.5 ) $\times 10^{-3}$	E2/M1
580.57 $\pm$ 0.10	5.80 $\pm$ 0.16	18.0 $\pm$ 2.5	( 1.34 $\pm$ 0.19 ) $\times 10^{-3}$	M1
608.29 $\pm$ 0.10	2.44 $\pm$ 0.08	4.5 $\pm$ 0.5	( 7.9 $\pm$ 0.9 ) $\times 10^{-4}$	E1
627.72 $\pm$ 0.10	39.5 $\pm$ 1.0	56 $\pm$ 3	( 6.1 $\pm$ 0.4 ) $\times 10^{-4}$	E1
644.82 $\pm$ 0.24	13.8 $\pm$ 0.4	37.5 $\pm$ 2.5	(11.7 $\pm$ 0.8 ) $\times 10^{-4}$	
645.87 $\pm$ 0.17				
703.33 $\pm$ 0.10	18.7 $\pm$ 0.5	43 $\pm$ 2	( 9.9 $\pm$ 0.5 ) $\times 10^{-4}$	M1
709.90 $\pm$ 0.10	3.18 $\pm$ 0.09	7.5 $\pm$ 2.0	( 1.02 $\pm$ 0.27 ) $\times 10^{-3}$	M1/E2
777.37 $\pm$ 0.10	27.22 $\pm$ 0.66	59 $\pm$ 5	( 9.3 $\pm$ 0.8 ) $\times 10^{-4}$	E2/M1
826.02 $\pm$ 0.13	4.08 $\pm$ 0.10	3 $\pm$ 1	( 0.32 $\pm$ 0.11 ) $\times 10^{-3}$	E1
833.72 $\pm$ 0.18	7.12 $\pm$ 0.22	10.5 $\pm$ 0.7	( 6.4 $\pm$ 0.5 ) $\times 10^{-4}$	
835.67 $\pm$ 0.22				
1024.04 $\pm$ 0.10	4.62 $\pm$ 0.11	4.4 $\pm$ 0.4	( 4.1 $\pm$ 0.4 ) $\times 10^{-4}$	M1
1076.63 $\pm$ 0.10	100	100	4.32 $\times 10^{-4}$ <sup>b</sup>	E2
1153.05 $\pm$ 0.10	37.02 $\pm$ 1.06	32 $\pm$ 2	( 3.73 $\pm$ 0.26 ) $\times 10^{-4}$	E2/M1
1163.03 $\pm$ 0.10	1.43 $\pm$ 0.05	4.7 $\pm$ 2.5	( 1.4 $\pm$ 0.8 ) $\times 10^{-3}$	E2/M1
1253.11 $\pm$ 0.10	1.86 $\pm$ 0.06	0.8 $\pm$ 0.2	( 1.8 $\pm$ 0.5 ) $\times 10^{-4}$	E1
1349.15 $\pm$ 0.10	3.56 $\pm$ 0.11	2.0 $\pm$ 0.3	( 2.4 $\pm$ 0.4 ) $\times 10^{-4}$	E2/M1
1801.70 $\pm$ 0.10	2.00 $\pm$ 0.06	0.6 $\pm$ 0.2	( 1.3 $\pm$ 0.4 ) $\times 10^{-4}$	E2/M1
1854.38 $\pm$ 0.13	20.8 $\pm$ 0.6	7.1 $\pm$ 1.1	( 1.47 $\pm$ 0.23 ) $\times 10^{-4}$	E2/M1
1920.72 $\pm$ 0.13	25.2 $\pm$ 0.7	4.2 $\pm$ 0.8	( 0.72 $\pm$ 0.14 ) $\times 10^{-4}$	E1

<sup>a</sup>Normalized to  $4.32 \times 10^{-4}$  for the 1076.63-keV  $\gamma$  ray.

<sup>b</sup>Theoretical value from Ref. 8.





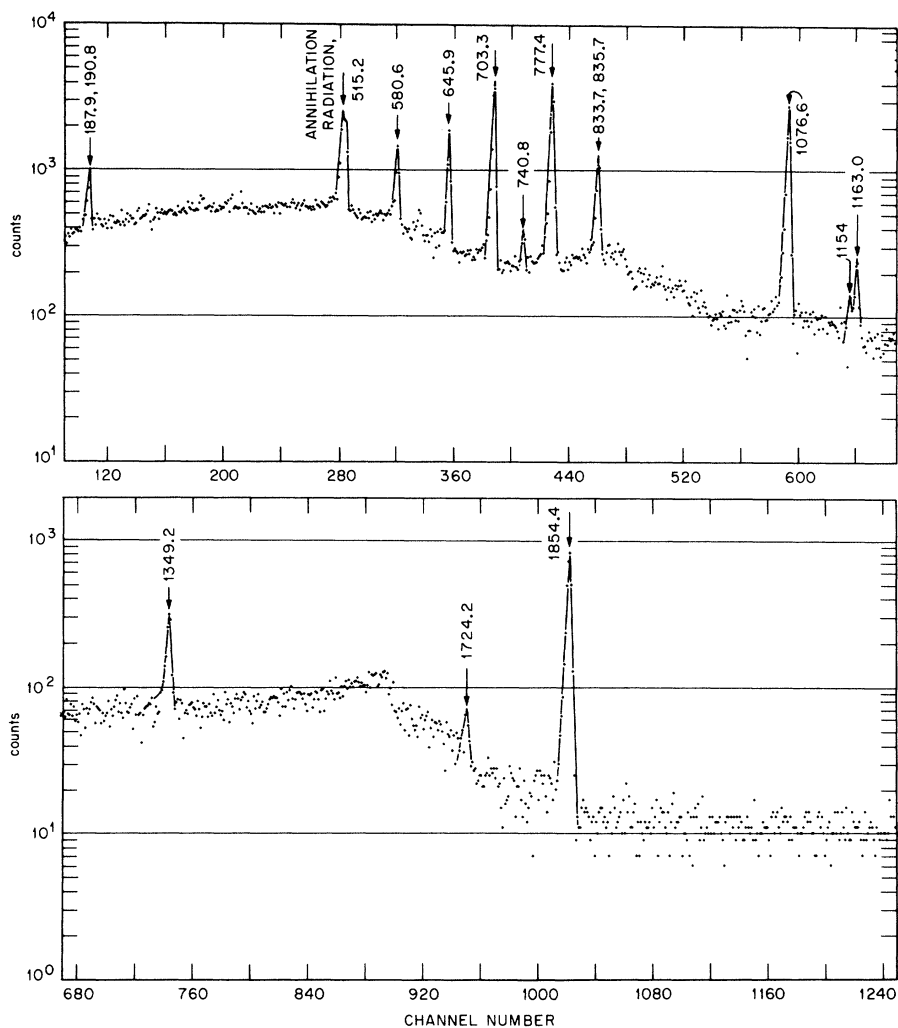


FIG. 14. Coincidence spectrum obtained with the gate set on the 627.7-keV peak; taken with system (c) (see text).

With the coincidence gate set on 443.13-keV  $\gamma$  ray, the 1253.11-keV transition appears relatively intense in the spectrum. In addition, this  $\gamma$  ray is seen in the spectra gated by the 1076.63-keV transition. These data establish the placement of this transition as feeding the 2672.76-keV level from a level at  $2672.76 + 1253.11 = 3925.87$  keV.

When the gate is set on the 1153.05-keV  $\gamma$  ray (see Fig. 15), a strong coincidence peak is seen at 1696.25 keV. A similarly strong coincidence relationship with this transition is not observed for any other gate except that at 1076.63 keV. These data are easily explained by placing this transition between the previously established 3925.89- and 2229.68-keV levels. Similar arguments hold for the 1296.03-keV transition observed in the spectrum coincident with the 443.13-keV gate to establish a level at  $2672.76 + 1296.03 = 3968.79$  keV.

The coincidence spectra discussed above disclose some of the basic features of the level scheme of  $^{86}\text{Sr}$  on which to build a detailed level scheme. In all, about 40 coincidence spectra were obtained, and a complete discussion of the coincidence results will be given in the next section, where the evidence for the individual levels is presented.

The  $\beta^+$  and electron-capture feeding to the levels as deduced from our  $\gamma$ -ray intensity balances and the  $\log ft$  values of the  $\beta^+$  and/or electron-capture feeding are shown in Table VI. The  $\beta^+/\text{EC}$  ratios were taken from the *Table of Isotopes*.<sup>9</sup>

The proposed level scheme of  $^{86}\text{Sr}$  is shown in Fig. 24, but before discussing the individual levels we point out that recent ( $p, p'$ ) work<sup>10</sup> on this nucleus has indicated levels at the following energies: 1077, 1854, 2229, 2481, 2645, 2671, 2788, 2879, 2997, 3055, 3185, 3317, 3362, 3432, 3499, 3552, 3645, 3686, 3769, and 3925 keV.



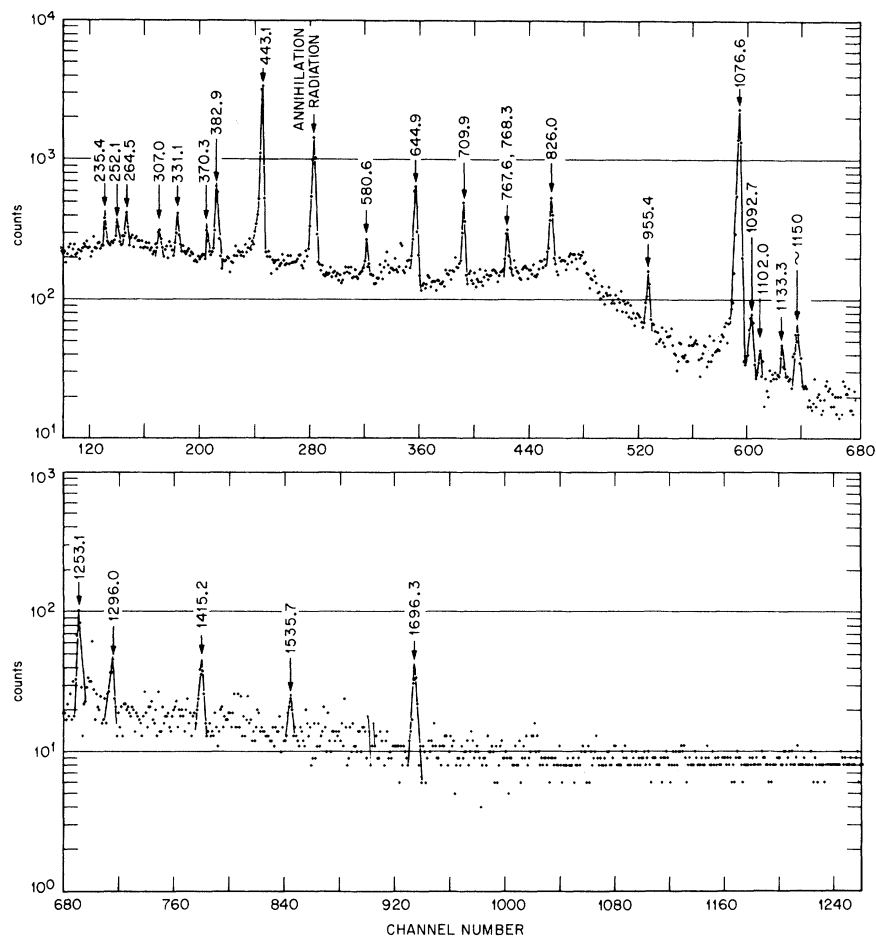


FIG. 15. Coincidence spectrum obtained with the gate set on the 1153-keV peak; taken with system (c) (see text).

## VII. DECAY SCHEME OF $^{86}\text{Y}$

### A. $^{86}\text{Y}$ Ground State— $4^-$

The positron branch from  $^{86}\text{Y}$  to the first  $2^+$  level in  $^{86}\text{Sr}$  has a  $\Delta J=2$ , yes character. Since there is no positron feeding to the ground state,<sup>4</sup> a spin-parity of  $4^-$  is most likely for the  $^{86}\text{Y}$  ground state. This assignment agrees with Nordheim's "strong rule."

### B. $1076.63 \pm 0.10$ -keV Level — $2^+$

This level as well as its spin-parity assignments of  $2^+$  was unambiguously determined from the decay of  $^{86}\text{Rb}$ .<sup>11</sup> In the present work the position of this level is confirmed by the spectrum taken in coincidence with the 1076.63-keV line. Except for a few transitions, this coincidence spectrum is similar to the singles  $\gamma$ -ray spectrum (compare Figs. 2 and 3 with Fig. 1).

### C. $1854.20 \pm 0.10$ -keV Level — $2^+$

The evidence to establish this level has already

been discussed in Sec. VI C. Additional evidence is obtained from the difference between the first and second positron branches<sup>4</sup> of  $818 \pm 56$  keV. The experimental  $K$  conversion coefficients of the 1854.38- and the 777.37-keV lines indicate  $E2$  and/or  $M1$  multipolarity, so spins and parity of  $1^+$  and  $2^+$  are allowed. The  $\log ft$  value of 8.8 calculated for the  $\beta^+$  branch feeding this level is in accord with the values generally obtained for unique first-forbidden transitions, so  $1^+$  is excluded.

### D. $2229.68 \pm 0.14$ -keV Level — $4^+$

Some evidence for this level has been discussed previously in Sec. VI D. An energy difference of  $1134 \pm 45$  keV between the first and third positron branches<sup>4</sup> provides further support for this level.

The  $E2/M1$  nature of the 1153.05-keV transition shows that the parity of this level is positive. The 1076.63–1153.05-keV  $\gamma$ - $\gamma$  directional correlation<sup>4</sup> restricts the possible spin values to 2, 3, and 4. A spin of 2 for this level is excluded, since the  $\log ft$  value of 7.7 for the positron branch that feeds it is in line with that expected for a nonunique

TABLE VI. Level energies,  $\beta^+$  and electron-capture feeding, and  $\log ft$  values for the decay of  $^{86}\text{Y}$  to levels in  $^{86}\text{Sr}$ . The feeding and  $\log ft$  values were deduced from  $\gamma$ -ray intensities. Essentially all of the transitions are placed in the decay scheme so that the level feedings are not subject to errors from unplaced transitions.

Level energy	$\beta^+$ feeding (%)	Electron-capture feeding (%)	$\log ft^a$
1076.63	1.9 $\pm$ 2.9	0.1 $\pm$ 0.2	8.8
1854.20	1.05 $\pm$ 1.00	0.14 $\pm$ 0.13	8.40
2229.68	3.9 $\pm$ 0.9	0.7 $\pm$ 0.2	7.7
2481.91	1.8 $\pm$ 0.7	0.7 $\pm$ 0.2	7.7
2642.27	0.05 $\pm$ 0.03	0.03 $\pm$ 0.02	9.0
2672.76	5.0 $\pm$ 0.5	3.7 $\pm$ 0.2	7.0
2788.4	0.03 $\pm$ 0.04	0.03 $\pm$ 0.04	8.9
2878.28	0.79 $\pm$ 0.10	0.50 $\pm$ 0.06	7.7
2997.34	13.7 $\pm$ 0.3	11.7 $\pm$ 0.2	6.3
3055.66	1.51 $\pm$ 0.12	1.51 $\pm$ 0.12	7.1
3185.19	1.71 $\pm$ 0.51	2.56 $\pm$ 0.76	6.8
3291.08	0.03 $\pm$ 0.02	0.06 $\pm$ 0.04	$\approx$ 8.4 <sup>b</sup>
3317.58	1.5 $\pm$ 0.2	3.2 $\pm$ 0.5	6.6
3362.06	0.25 $\pm$ 0.03	0.64 $\pm$ 0.07	7.3
3499.84	0.01 $\pm$ 0.04	0.08 $\pm$ 0.19	$\approx$ 7.3 <sup>b</sup>
3555.66	...	...	...
3644.94	0.44 $\pm$ 0.03	4.44 $\pm$ 0.27	6.4
3686.74	0.08 $\pm$ 0.01	1.13 $\pm$ 0.09	6.9
3765.59	0.40 $\pm$ 0.02	9.00 $\pm$ 0.42	6.0
3774.80	0.02 $\pm$ 0.01	0.41 $\pm$ 0.05	7.3
3831.06	0.4 $\pm$ 0.1	14.3 $\pm$ 1.3	5.7
3871.53	...	0.36 $\pm$ 0.03	7.3
3925.89	...	6.83 $\pm$ 0.11	6.0
3942.41	...	0.80 $\pm$ 0.08	7.0
3968.84	...	1.40 $\pm$ 0.09	6.7
4146.0	...	0.73 $\pm$ 0.05	6.9
4206.0	...	0.88 $\pm$ 0.08	6.7
4339	...	...	...
4410.5	...	0.20 $\pm$ 0.02	7.3
4718	...	0.12 $\pm$ 0.04	7.0
4954	...	0.06 $\pm$ 0.05	$\approx$ 6.8 <sup>b</sup>

<sup>a</sup>The  $K$ -capture-to-positron ratios were obtained from the *Table of Isotopes* (Ref. 9), and the  $\log ft$  values were not corrected for first-forbidden unique transitions.

<sup>b</sup>The  $\log ft$  values have large uncertainties due to weak feeding of the level.

first-forbidden transition. A spin of 4 is consistent with recent  $\gamma$ - $\gamma$  directional-correlation work.<sup>12</sup>

#### E. 2481.91 $\pm$ 0.10-keV Level - 3<sup>-</sup>

Evidence for this level has been presented in Sec. VI C. Also the 252.05-keV line is observed to be in coincidence with 1153.05- and 1076.63-keV  $\gamma$  rays. The energy sum relationships obtained for the placement of the 252.05- and 627.72-keV  $\gamma$  rays are excellent:

$$(2229.68 \pm 0.14) + (252.05 \pm 0.13) = 2481.73 \pm 0.18 \text{ keV}$$

and

$$(1854.20 \pm 0.10) + (627.72 \pm 0.10) = 2481.92 \pm 0.14 \text{ keV.}$$

The  $E1$  character of the 627.72- and 252.05-keV  $\gamma$  rays uniquely establishes the spin and parity as 3<sup>-</sup> for the 2481.91-keV level. The 2482.08-keV  $\gamma$  ray has been interpreted<sup>3</sup> as an  $E3$  transition from this level to the  $^{86}\text{Sr}$  ground state.

#### F. 2642.27 $\pm$ 0.28-keV Level - (2)<sup>+</sup>

A level at 2642  $\pm$  5 keV was observed in the recent  $^{86}\text{Sr}(p, p')$  work of Ramayya *et al.*<sup>10</sup> There was little indication that the 2641.9-keV transition observed in the singles spectrum of Fig. 24 is in coincidence with the 1076.63-keV line, but the upper limit on its intensity with that gate could allow feeding to the 1854.2-keV level, which has a strong ground-state branch. If we place a level at 2642.27 keV, we can account for the 355.07-keV line as the transition between this level and the level at 2997.34 keV. There is some indication in the coincidence spectra that the 355.07-keV  $\gamma$  ray is in coincidence with the 2641.9-keV  $\gamma$  ray. Because the primary decay of this level is to the ground state, the possible values for spin and parity are 1<sup>+</sup> and 2<sup>+</sup>. The  $\log ft$  value of 9.0 is too low to allow 1<sup>+</sup>.

#### G. 2672.76 $\pm$ 0.13-keV Level - 5<sup>-</sup>

Evidence to establish the existence of this level was presented in Sec. VI D. Furthermore, the 443.13-keV transition shows up strongly in  $\beta$ - $\gamma$  coincidence spectra taken at  $E_{\beta^+} = 1278$  keV.<sup>4</sup> The 2672.76-keV level makes it possible to place the 190.80-keV  $\gamma$  ray between the 2672.76- and 2481.91-keV levels. The position of the 190.80-keV  $\gamma$  ray is further confirmed by the fact that this  $\gamma$  ray is not in coincidence with the 443.13-keV  $\gamma$  ray, but is strongly in coincidence with the 627.72-, 777.37-, 1854.38-, and 1076.63-keV transitions.

The  $E1$  nature of the 443.13-keV  $\gamma$  ray establishes odd parity and restricts the possible spin values of the 2672.76-keV level to 2, 3, 4, or 5. A 2<sup>-</sup> assignment is excluded by the  $\log ft$  value of 7.0. A spin of 3 is improbable in view of the absence of additional  $E1$  transitions to the 1076.6- and 1854.2-keV 2<sup>+</sup> levels. The  $E2$  character of the 190.80-keV line is in agreement with an assignment of 4<sup>-</sup> or 5<sup>-</sup>. A spin of 5 has been verified in very recent  $\gamma$ - $\gamma$  correlation studies.<sup>12</sup>

#### H. 2788.2 $\pm$ 0.7-keV Level

Recent work<sup>10</sup> on  $^{86}\text{Sr}(p, p')^{86}\text{Sr}$  has revealed a level at 2790  $\pm$  5 keV. If we assume that this level decays to the 1076.63-keV level, then this decay

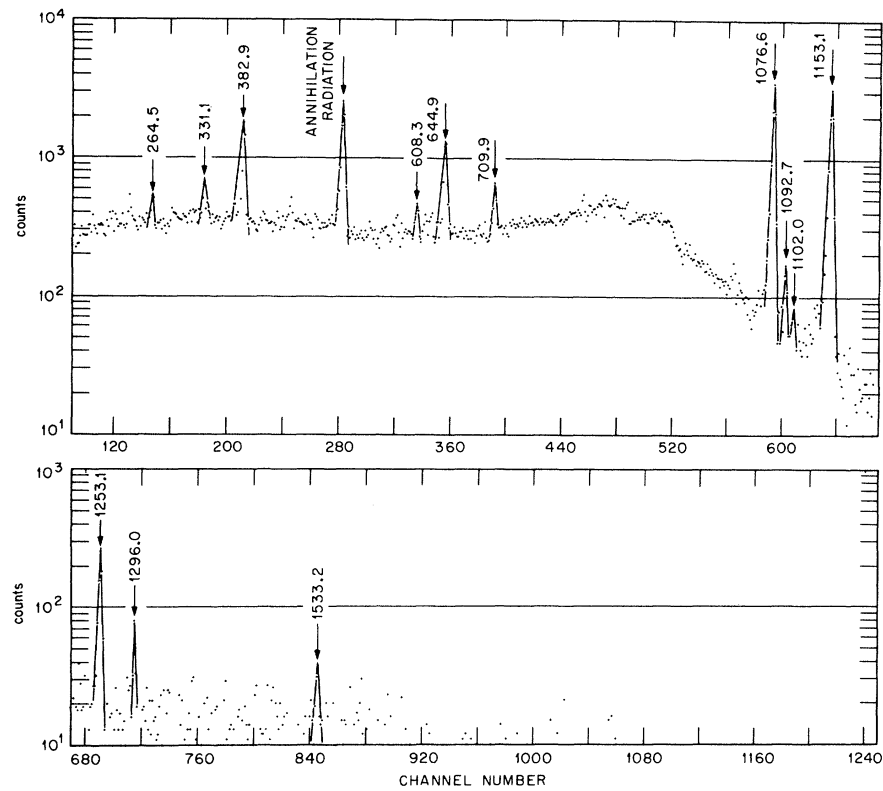


FIG. 16. Coincidence spectrum obtained with the gate set on the 442-keV peak; taken with system (c) (see text).

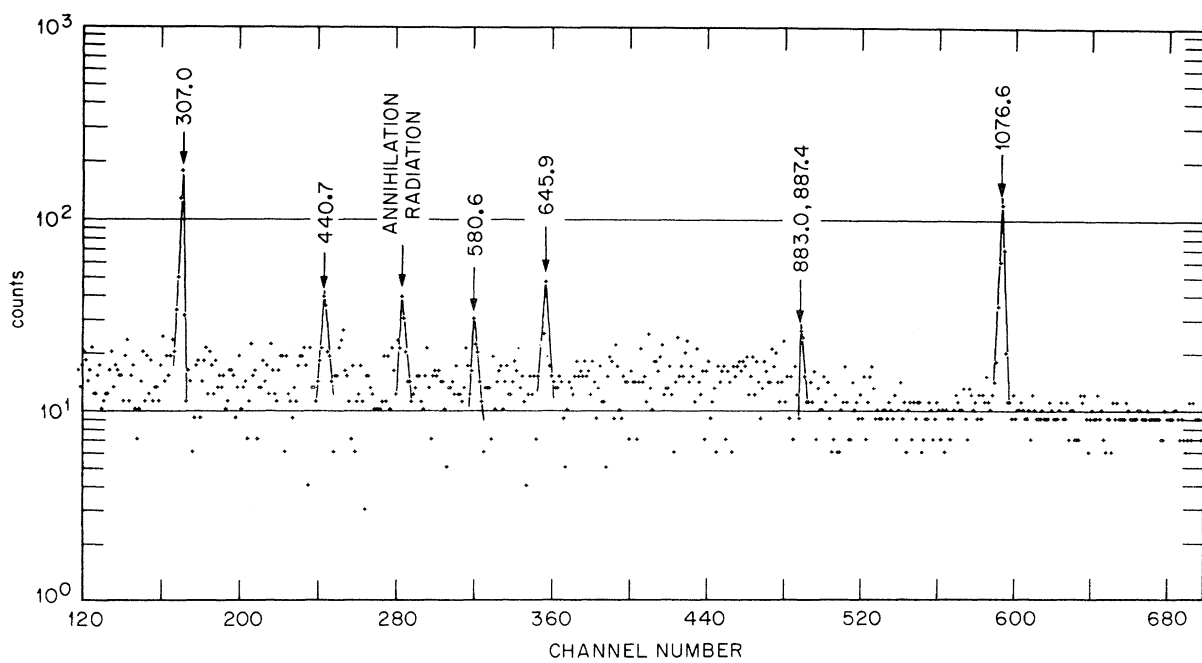


FIG. 17. Coincidence spectrum obtained with the gate set on the 1801.7-keV peak; taken with system (c) (see text).

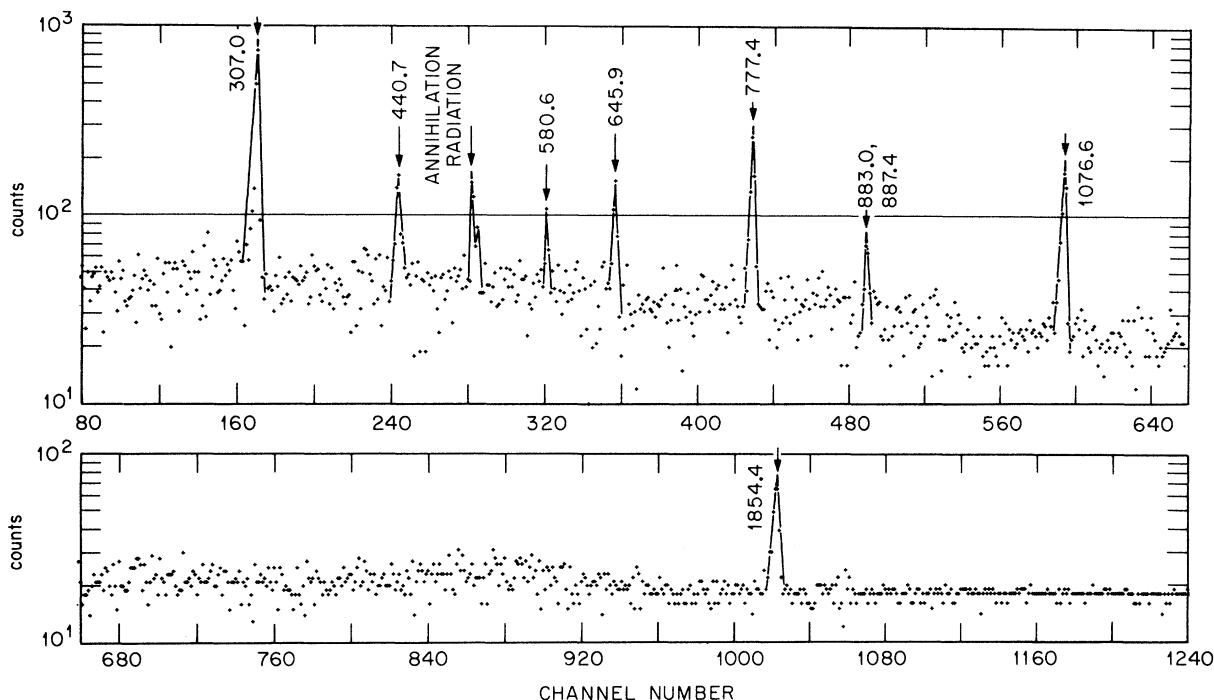


FIG. 18. Coincidence spectrum obtained with the gate set on the 1024.0-keV peak; taken with system (c) (see text).

must take place by a  $\gamma$  ray of energy  $1709 < E_\gamma < 1719$  keV. Only the 1711.6-keV  $\gamma$  ray satisfies this condition. The 2790.0-keV  $\gamma$  ray is placed as the transition from the 2788.2-keV level to the ground state. Nothing can be said about this level from the coincidence spectra, because of the very low intensity of the 1711.6-keV transition. Because of the tenuous nature of the evidence of population of this level in the decay of  $^{86}\text{Y}$ , it is shown dashed in Fig. 24.

#### I. $2878.28 \pm 0.10$ -keV Level - $3^+, 4^+$

This level is established by the observed coincidence relationships between the 1024.04  $\rightarrow$  1854.38 and 1801.70  $\rightarrow$  1076.63-keV  $\gamma$  rays (see Figs. 17 and 18). The sum energies (in keV) of these cascades agree with each other within the limits of error:

$$(1024.04 \pm 0.10) + (1854.38 \pm 0.13) = 2878.42 \pm 0.16;$$

$$(1801.70 \pm 0.10) + (1076.63 \pm 0.10) = 2878.33 \pm 0.14.$$

This level enables the placement of a weak line observed in the singles spectrum at an energy of  $648.6 \pm 1.0$  keV as a transition from the 2229.68-keV level. The position of this line also explains the coincidences observed between the 307.00- and 1153.05-keV transitions (see Fig. 15).

The  $M1$  and/or  $E2$  nature of the 1024.04- and 1801.70-keV transitions establishes even parity

for this level and restricts the possible spins to from zero to four. The  $\log ft$  value of 7.8 for the  $\beta^+$  branch feeding eliminates 0, 1, and 2.

#### J. $2997.34 \pm 0.11$ -keV Level - $3^-$

A discussion of the evidence for this level was presented in Sec. VI B. From energy fits the 767.63-, 515.18-, 1142.3-, and 2997.6-keV  $\gamma$  rays can be placed as depopulating this level. The positions of the 515.18- and 767.63-keV lines as originating at this level are consistent with the coincidence results in Table V. The following energy sum relations (in keV) agree very well with one another:

$$(1076.63 \pm 0.10) + (1920.72 \pm 0.13) = 2997.35 \pm 0.16,$$

$$(1854.20 \pm 0.10) + (1142.3 \pm 1.0) = 2996.5 \pm 1.0,$$

$$(2481.91 \pm 0.10) + (515.18 \pm 0.20) = 2997.09 \pm 0.23.$$

Coincidence relations indicate that the line observed at 767 keV is a doublet. We have deduced the transition energy, 767.63 keV, from the energy difference between the  $(2997.34 \pm 0.11)$ - and  $(2229.68 \pm 0.14)$ -keV levels. The 1142.3  $\pm$  1.0-keV  $\gamma$  ray is indicated in the decay scheme as a dashed line, since its position is exclusively based on energy considerations and its energy is poorly known. The 689.29-keV transition can also be placed on an energy fit between this level and the 3686.74-keV level, but it also fits between levels at 2672.76

and 3362.05 keV. The spectrum gated on the 1920.72-keV transition favors the latter assignment.

The  $E1$  nature of the 1920.72-keV line yields a  $(1-3)^-$  assignment, the  $M1/E2$  nature of the 515.18-keV  $\gamma$  ray gives a  $(1-5)^-$  assignment, and the  $\log ft$  value of 6.3 yields a  $(3-5)^-$  assignment for this level. So the spin and parity of the 2997.34-keV level is assigned as  $3^-$ .

#### K. $3055.66 \pm 0.17$ -keV Level - $(4, 5)^-$

The  $\gamma$ - $\gamma$  coincidence experiments summarized in Table V show that the 826.02-keV line is in coincidence with the 1153.05- and 1076.63-keV  $\gamma$  rays (see Figs. 15 and 11). Table V also shows that the 382.86-keV line is coincident with the 443.13-, 1076.63-, and 1153.05-keV  $\gamma$  rays (see Figs. 11,

15, and 16). A level at 3055.66 keV which decays by 382.86- and 826.02-keV  $\gamma$  rays to the 2672.76- and 2229.68-keV levels, respectively, explains these coincidence results. Additional evidence for this level is obtained from the following energy sum relations in keV:

$$(2229.68 \pm 0.14) + (826.02 \pm 0.13) = 3055.70 \pm 0.19,$$

$$(2672.76 \pm 0.13) + (382.86 \pm 0.23) = 3055.62 \pm 0.27.$$

From the  $E1$  nature of the 826.02-keV  $\gamma$  ray, the parity is established as odd for this new level and  $J$  is limited to 2-5. However, the  $\log ft$  of 7.1 for the  $\beta$ -ray group feeding this level eliminates spin 2. In view of the absence of additional  $E1$  transitions to the lower-lying  $2^+$  levels, the spin and parity of the 3055.66-keV level are most probably  $(4, 5)^-$ .

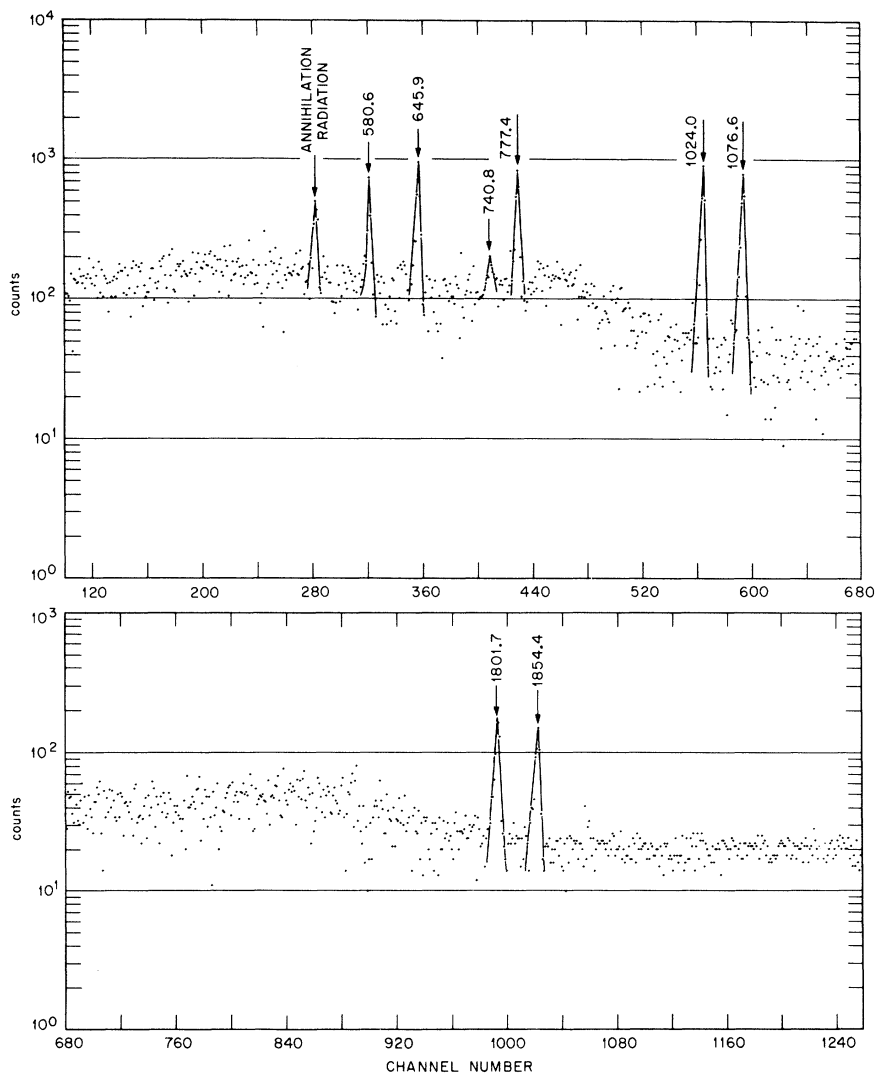


FIG. 19. Coincidence spectrum obtained with the gate set on the 307.0-keV peak; taken with system (c) (see text).

FIG. 20. Coincidence spectrum obtained with the gate set on the 703.3-keV gate; taken with system (c) (see text).

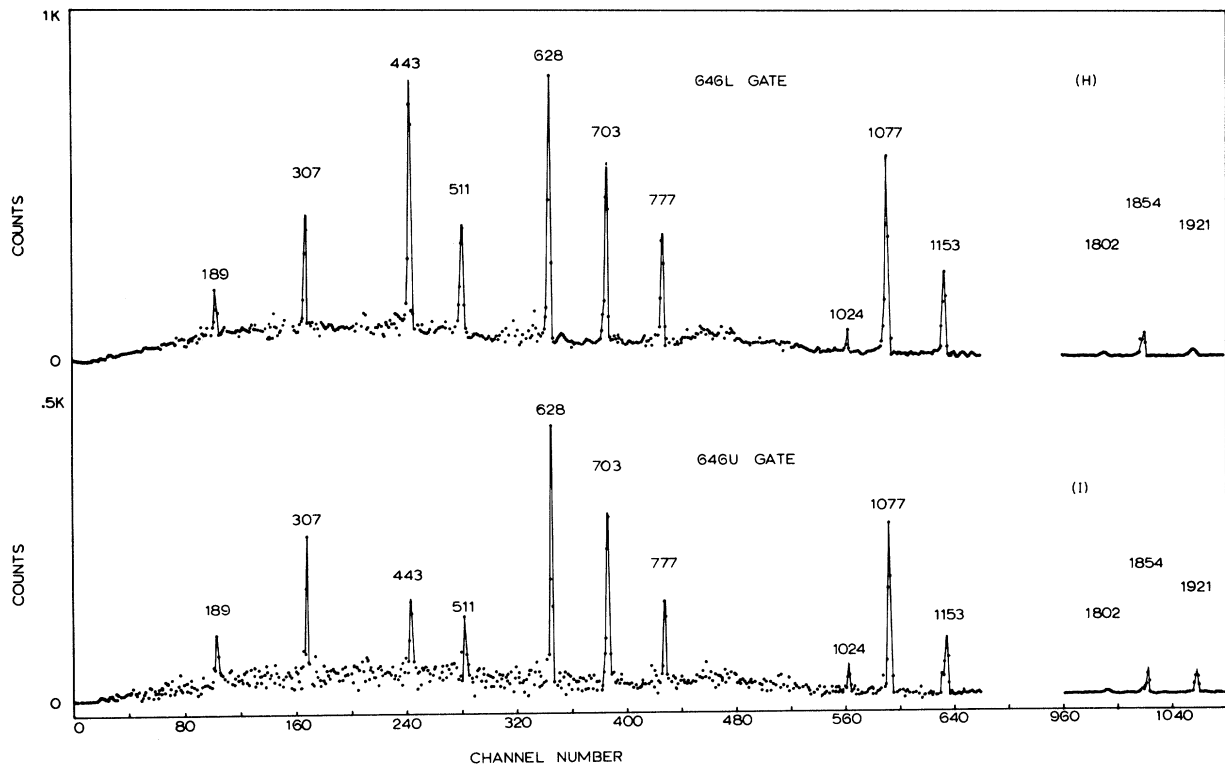
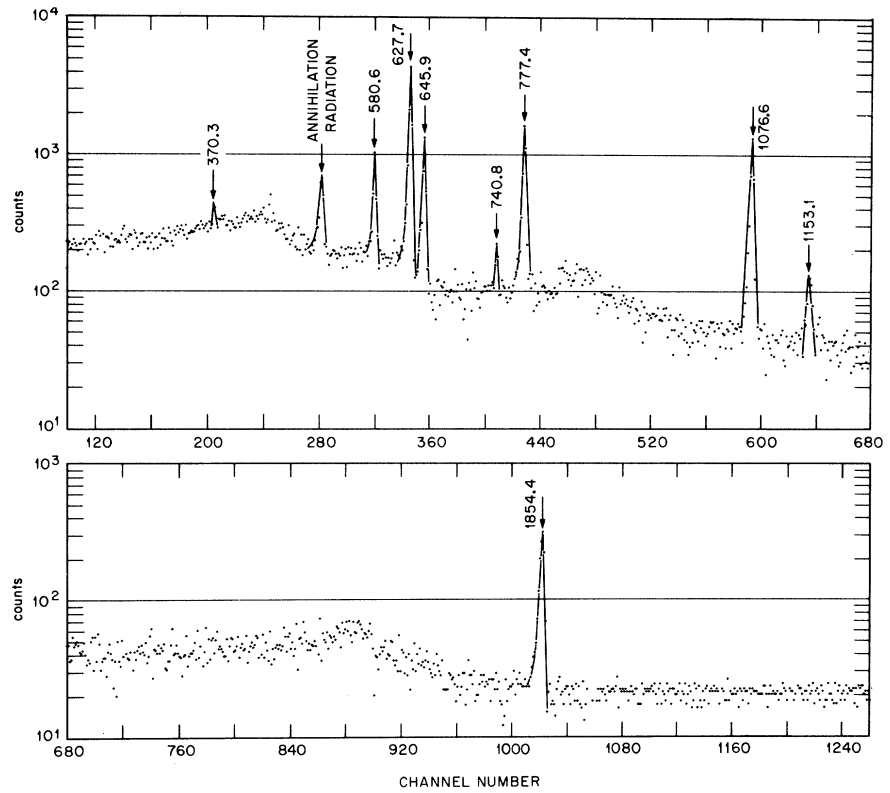


FIG. 21. Coincidence spectra obtained with the gate set on the lower side (H) of the 646-keV peak and with the gate set on the upper side (I) of the 646-keV peak. The spectra were taken with system (c) (see text).

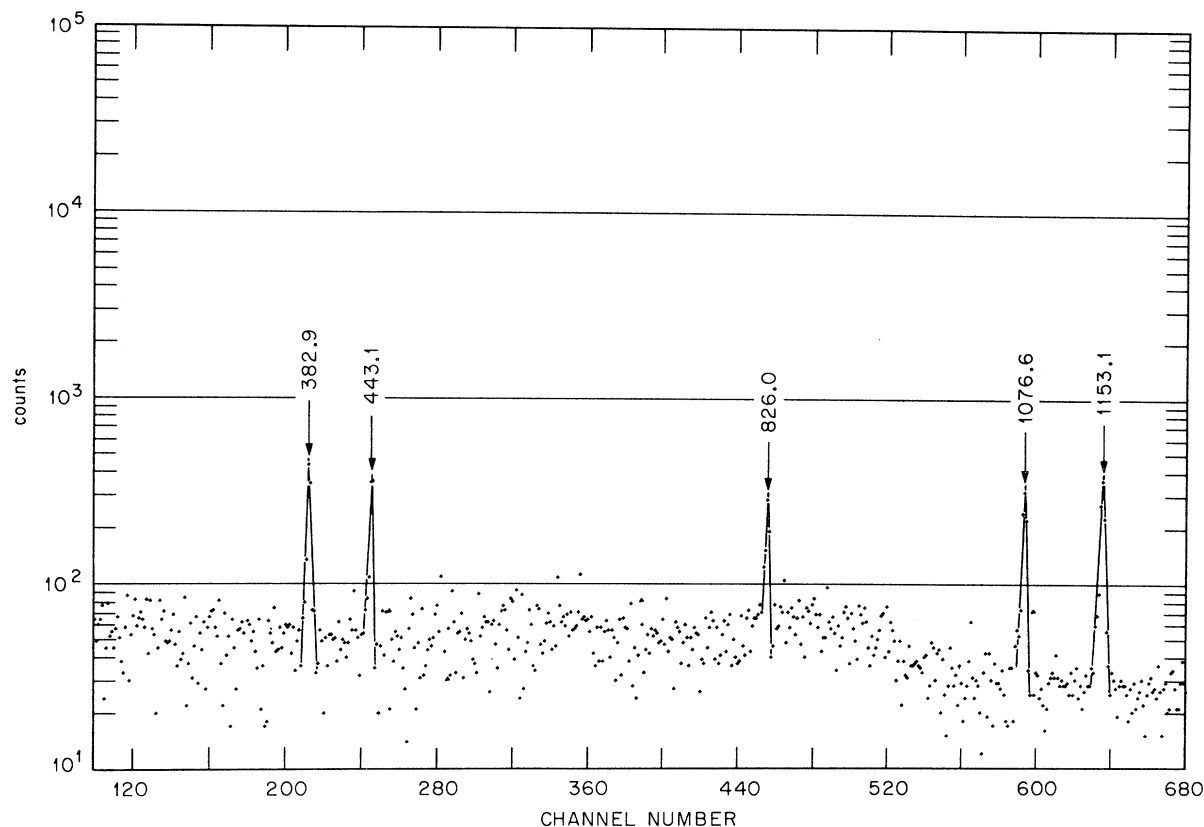


FIG. 22. Coincidence spectrum obtained with the gate set on the 709.9-keV peak; taken with system (c) (see text).

#### L. $3185.19 \pm 0.10$ -keV Level - ( $3^-$ )

A level at this energy accounts for the following experimentally determined coincidence results:

- (1) The 187.87-keV line is seen in coincidence with the 1920.72- and 1076.63-keV  $\gamma$  rays (see Table V, Figs. 11 and 12).
- (2) The 307.00-keV  $\gamma$  ray is in coincidence with 1024.04-, 1801.70-, 777.37-, 1076.63-, and 1854.38-keV  $\gamma$  rays (see Table V, Figs. 11, 13, 18, and 19).
- (3) The 703.33-keV  $\gamma$  ray is seen in coincidence with the 627.72-, 777.37-, 1076.63-, and 1854.38-keV lines (see Figs. 11, 13, 14, and 20, Table V).
- (4) The 955.35-keV line is seen in coincidence with the 1076.63-, and 1153.05-keV  $\gamma$  rays (see Table V, Figs. 11 and 15).

In addition to these coincidence results, the new level is supported by the following energy-sum relationships, with energies given in keV:

$$\begin{aligned} (2997.34 \pm 0.11) + (187.87 \pm 0.13) &= 3185.21 \pm 0.17, \\ (2878.28 \pm 0.10) + (307.00 \pm 0.10) &= 3185.28 \pm 0.14, \\ (2481.91 \pm 0.10) + (703.33 \pm 0.10) &= 3185.24 \pm 0.14, \\ (2229.68 \pm 0.14) + (955.35 \pm 0.20) &= 3185.03 \pm 0.25, \end{aligned}$$

$$(1076.63 \pm 0.10) + (2108.87 \pm 0.33) = 3185.50 \pm 0.35.$$

From the  $E1$  nature of the 307.00-keV line and the  $M1$  character of the 703.33-keV  $\gamma$  ray and the dipole character of the 187.87-keV transition, the spin and parity of this level are restricted to ( $2, 3$ , or  $4^-$ ). A  $2^-$  assignment can be excluded because of the positron feeding which has a  $\log ft$  of 6.8. The 2108.87-keV  $\gamma$  ray is placed as the transition from this level to the 1076.63-keV  $2^+$  level on the basis of energy considerations. If the position of the 2108.87-keV  $\gamma$  ray is correct, a spin of  $3^-$  is indicated.

#### M. $3291.08 \pm 0.17$ -keV Level

Evidence for this level rests primarily upon the observation that the 235.37-keV  $\gamma$  ray is in coincidence with the 1076.63-, 1153.05-, 443.13-, 382.86-, and 826.02-keV  $\gamma$  rays (see Table V). If this level at  $(3055.66 \pm 0.17) + (235.37 \pm 0.23) = 3291.03 \pm 0.29$  keV is introduced, two other transitions, namely, those at  $503.0 \pm 0.4$  and  $618.24 \pm 0.40$  keV, can be placed on the basis of energy relations to the levels at 2788.4 and 2672.76 keV, respectively. It is not possible to draw any further supporting evi-

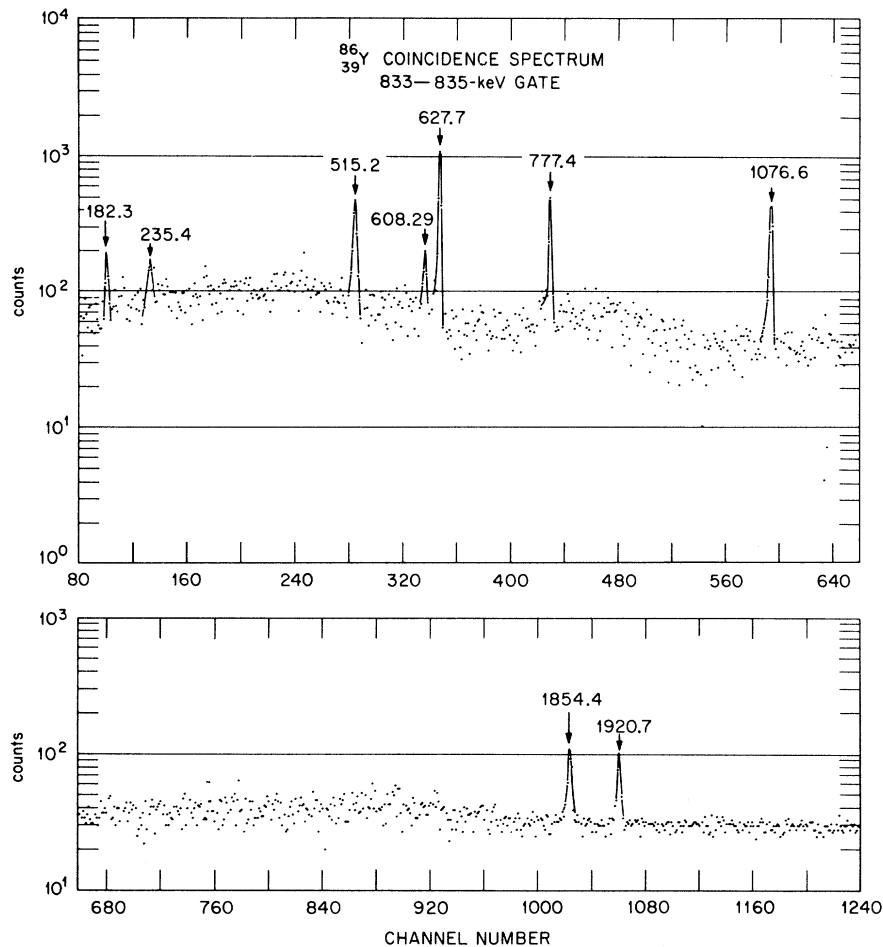


FIG. 23. Coincidence spectrum obtained with the gate set on the 835-keV peak; taken with system (c) (see text).

dence from the coincidence data in Table V, because of the weak intensity of these transitions. Further evidence for the existence of this level is provided by some of the transitions which feed it, as discussed later.

From the known spins of levels fed by this state, spins of 2 to 6 are allowed. The error on the intensity balances into and out of this level is so large that one cannot use the  $\log ft$  to seriously restrict the spin choices.

N.  $3317.58 \pm 0.20$ -keV Level—(3, 4, 5)<sup>-</sup> and the  
 $3831.06 \pm 0.14$ -keV Level—(4, 5)<sup>-</sup>

These two levels are based on a variety of inter-related arguments. A line at approximately 646 keV is seen in the coincidence spectra obtained with gates set on the 307.00-, 703.33-, and 443.13-keV lines. If the 646-keV transition is placed as cascading into the 3185.19-keV level, the coincidence relationship between the 443- and 646-keV lines cannot be explained, since no  $\gamma$  ray of reasonable intensity is seen to connect the 3185.19- and 2672.76-keV levels. Hence one must assume

that the 646-keV line is a doublet. This assumption is further supported by the fact that in the coincidence spectrum obtained with a narrow gate setting on the upper half of the 646-keV line (see Fig. 21), the 307.00-keV line is stronger relative to the 443.13-keV line, whereas in the spectrum obtained with a narrow gate setting on the lower half of the 646-keV line (see Fig. 21), the 443.13-keV transition is stronger relative to the 307.00-keV  $\gamma$  ray.

A line at 834 keV is seen in the coincidence spectrum obtained with the gate setting on the 1920.72-keV  $\gamma$  ray (see Fig. 12). This suggests that an 834-keV  $\gamma$  ray feeds the 2997.34-keV level. However, in that case one expects the 515.18- and 627.72-keV  $\gamma$  rays to have about equal intensities (the other  $\gamma$  rays which depopulate the 2481.9-keV level are very weak) in the coincidence spectrum taken with the gate set on 834 keV. From the coincidence spectrum in Fig. 23, it can be seen that in fact the 627.72-keV line is at least four times stronger than the 515.18-keV peak. This intensity difference cannot be ascribed to the double-escape



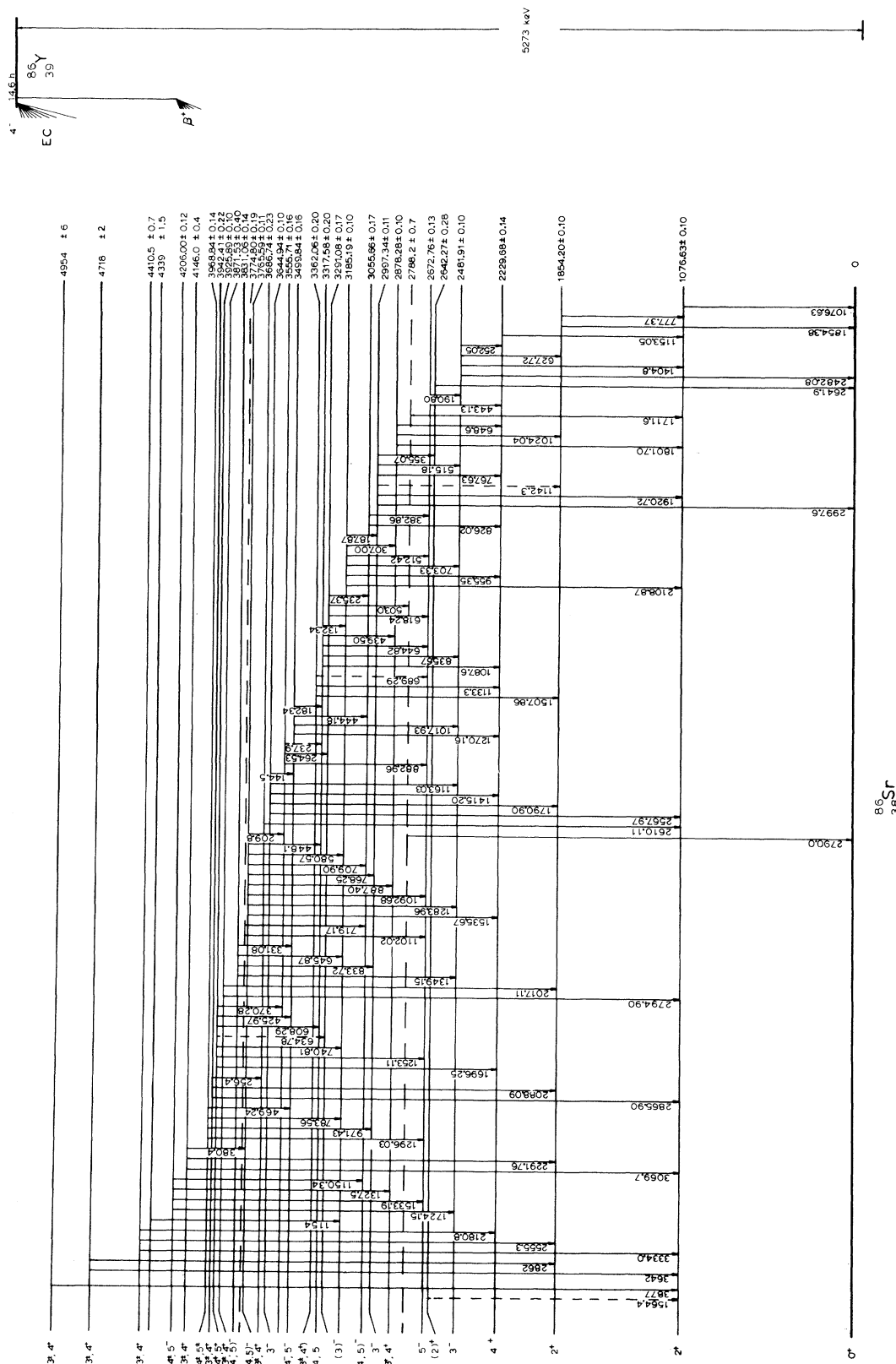


FIG. 24. Proposed  $^{86}\text{Y}$  decay scheme. The dashed levels and dashed transitions indicate cases for which there is only weak evidence. The information on the positron and electron-capture feeding is presented in Table VI.

peak of the 1854.38-keV  $\gamma$  ray (1854.38 - 1022.0 = 832.38 keV) contributing to the gate pulses, since a 703.33-keV peak is absent in the coincidence spectrum.

A solution to this problem is obtained by assuming that there is also a doublet at approximately 836 keV; one of the members should be in coincidence with the 515.18-keV line, but both members should be coincident with the 627.72-keV transition.

In order to explain the fact that the 1349.15-keV transition is in coincidence with the 627.72-, 777.37-, 1076.63-, and 1854.38-keV  $\gamma$  rays (see Table V), a level at 3831.06 keV must exist. This means that by introducing just one level at 3317.58 keV, the problems connected with the coincidence results for the 646- and 836-keV gates can be solved satisfactorily.

As we shall see in Sec. VII X, there exists a  $3925.87 \pm 0.17$ -keV level which is shown in the coincidence experiments to be depopulated by a  $608.29 \pm 0.10$ -keV  $\gamma$  ray. This transition makes it possible to determine a level energy of  $3317.58 \pm 0.20$  keV. Subsequently, the energies in keV of the members of the 836- and 646-keV doublets can be derived:

$$(3317.58 \pm 0.20) - (2672.76 \pm 0.13) = 644.82 \pm 0.17,$$

$$(3317.58 \pm 0.20) - (2481.91 \pm 0.10) = 835.67 \pm 0.22,$$

$$(3831.06 \pm 0.14) - (3185.19 \pm 0.10) = 645.87 \pm 0.17,$$

$$(3831.06 \pm 0.14) - (2997.34 \pm 0.11) = 833.72 \pm 0.18.$$

The measured energies of the composite 646- and 836-keV lines,  $645.6 \pm 0.3$  and  $835.8 \pm 0.3$  keV, suggest that the 645.87- and 835.67-keV members of the doublets are the most intense ones. Calculations from the coincidence spectra yield the following intensities (in parentheses) for the doublets: 644.82 (2.65); 645.87 (11.1); 833.72 (1.8); 835.67 (5.3). A peak appears at 440.7 keV in the coincidence spectra taken with the gates set on 1801.70 and 1024.04 keV (see Figs. 17 and 18). This can be explained by placing the weakly observed 439.5-keV  $\gamma$  ray as the transition connecting the 3317.58- and 2878.28-keV levels. The 3317.58-keV level allows the placement of the 132.34-keV  $\gamma$  ray as a transition to the 3185.19-keV level.

In the coincidence spectrum obtained by gating on the 1270.16-keV transition, an intense 331.08-keV  $\gamma$  ray was observed which can be explained by placing this  $\gamma$  ray as a transition from the 3831.06- to the 3499.84-keV level. This placement is also consistent with the energy sum rule, namely,  $(3499.84 \pm 0.16) + (331.08 \pm 0.23) = 3830.92 \pm 0.28$  keV.

From the  $M1/E2$  character of the 1349.15-keV  $\gamma$  ray, the spin and parity of the 3831.06-keV level are established as  $(1-5)^-$ . The  $\beta$  feeding to this level is almost certainly allowed with a  $\log ft$  of

5.7 (the lowest of all the  $\log ft$  values) and therefore the permissible spin-parity assignments are  $3^-$ ,  $4^-$ , or  $5^-$ . Since the 3831.06-keV level is not observed to feed the low-lying  $2^+$  states,  $4^-$  and  $5^-$  are the most probable choices for the spin-parity assignments to this level.

A spin of 3, 4, or 5 is allowed for the 3317.58-keV level, since the  $\log ft$  value of 6.6 for the  $\beta$ -ray branch to this level indicates an allowed or first-forbidden nonunique process.

#### O. 3362.06-keV Level - $3^+$ , $4^+$

Strong coincidences are observed for the 1133.3-keV  $\gamma$  ray with both the 1153.05- and 1076.63-keV transitions. In the spectrum gated on the weak 1133.3-keV transition, the 443-keV  $\gamma$  ray seen there can be explained by a small contribution from the 1153-keV transition in the gate. Weak  $\gamma$  rays of 1507.86 and 689.29 keV (an alternate placement of the 689.29-keV transition was discussed in Sec. VII J) can be placed from this level. There exists marginal evidence for the coincidence of the 1507.86-keV transition with the 777.37- and 1853.03-keV gates. With these placements, the following energy sums (in keV) are obtained:

$$(1854.20 \pm 0.10) + (1507.86 \pm 0.20) = 3362.06 \pm 0.20,$$

$$(2229.68 \pm 0.14) + (1133.3 \pm 1.0) = 3363.0 \pm 1.0,$$

$$(2672.76 \pm 0.13) + (689.29 \pm 0.15) = 3362.05 \pm 0.20.$$

The first two sums are taken for the level energy because of the uncertainty in the placement of the 689.29-keV transition. A level at this energy also was seen recently in the  $^{86}\text{Sr}(p, p')^{86}\text{Sr}$  experiment cited earlier.<sup>10</sup>

The  $\log ft$  value of 7.3 for  $\beta$  decay to this level indicates that this feeding is either allowed or first-forbidden nonunique, which allows spin-parity assignments of  $(3, 4, 5)^+$ . The  $4^-$ ,  $5^+$  possibilities are excluded, since this level decays to the second  $2^+$  state.

#### P. 3499.84 $\pm$ 0.16-keV Level - $3^-$ , $4^-$ , $5^-$

With a gate setting of 1270.16 keV, the 1076.63- and 1153.05-keV transitions are observed prominently in the coincidence spectrum. These data indicate that the 1270.16-keV  $\gamma$  ray feeds the 2229.68-keV level from a level at  $3499.84 \pm 0.19$  keV. This level makes it possible to place the 1017.93- and 182.34-keV  $\gamma$  rays as transitions from this level to the 2481.91- and 3317.58-keV levels, respectively. The energy sums, in keV, are:

$$(2229.68 \pm 0.14) + (1270.16 \pm 0.13) = 3499.84 \pm 0.19,$$

$$(2481.91 \pm 0.10) + (1017.93 \pm 0.23) = 3499.84 \pm 0.25,$$

$$(3317.58 \pm 0.20) + (182.34 \pm 0.20) = 3499.92 \pm 0.29.$$

In the coincidence spectrum gated by 444.18 keV (see Fig. 16), the 443-, 331.08-, and 826.02-keV  $\gamma$  rays are observed. These coincidences indicate the existence of a 444.18-keV transition between the 3499.84- and 3055.66-keV levels. Further evidence of this is supplied by the observation of a  $\gamma$  ray at about 443 keV in the coincidence spectrum gated by 826.02 keV and by the requirements for intensity balance of this level.

Since the 331.08-keV  $\gamma$  ray from the 3831.06-keV odd-parity level discussed above has an  $M1/E2$  character, the parity of the 3499.84-keV level is established as odd. The  $\beta$ -decay branch to this level has a  $\log ft$  value of 7.7, which is compatible with an allowed or first-forbidden nonunique transition. Since the parity is restricted to be odd, the transition is allowed and the spin must be 3, 4, or 5.

#### Q. 3555.71 $\pm$ 0.16-keV Level

This level is introduced on the basis of the following energy sum (in keV) relationships:

$$(2672.76 \pm 0.13) + (882.96 \pm 0.17) = 3555.72 \pm 0.22,$$

$$(3291.08 \pm 0.17) + (264.53 \pm 0.13) = 3555.61 \pm 0.22,$$

$$(3317.58 \pm 0.20) + (237.9 \pm 0.3) = 3555.48 \pm 0.36.$$

In addition to the above energy sum relationships, a level at 3555  $\pm$  10 keV was observed in recent ( $p, p'$ ) work on  $^{86}\text{Sr}$ .<sup>10</sup> It should be pointed out that there is only marginal evidence from the coincidence data for the above placement of the 237.9- and 264.53-keV  $\gamma$  rays from this level. No statement can be made about the spin or parity from the available data.

#### R. 3644.94 $\pm$ 0.10-keV Level – 3<sup>-</sup>

This level accounts for the following observed coincidence relations: the 2567.97-keV  $\gamma$  ray coincident with the 1076.63-keV  $\gamma$  ray (see Fig. 11); the 1790.90-keV  $\gamma$  ray coincident with the 1854.38-keV  $\gamma$  ray (see Fig. 13); the 1415.20-keV  $\gamma$  ray coincident with the 1153.05- and 1076.63-keV  $\gamma$  rays (see Fig. 15); and the 1163.03-keV  $\gamma$  ray coincident with the 627.72-, 777.37-, 1076.63-, and 1854.38-keV  $\gamma$  rays. The 2580-keV peak seen in coincidence with 1076-keV  $\gamma$  ray (Fig. 9) is a composite of 2567.97- and 2610.11-keV  $\gamma$  rays, and both are in coincidence with the 1076-keV photopeak. In addition, the following energy relations (in keV) give added evidence for the existence of this level:

$$(1076.63 \pm 0.10) + (2567.97 \pm 0.18) = 3644.60 \pm 0.21,$$

$$(1854.20 \pm 0.10) + (1790.90 \pm 0.10) = 3645.10 \pm 0.14,$$

$$(2229.68 \pm 0.14) + (1415.20 \pm 0.23) = 3644.88 \pm 0.27,$$

$$(2481.91 \pm 0.10) + (1163.03 \pm 0.10) = 3644.94 \pm 0.14.$$

The weighted mean calculated for the level energy is 3644.94  $\pm$  0.10 keV.

A  $\log ft$  value of 6.4 for the  $\beta^+$  branch to this level is consistent with an allowed or first-forbidden nonunique decay to limit the spin to 3, 4, or 5. Since this level feeds lower-lying 2<sup>+</sup> and 3<sup>-</sup> levels, the spin and parity assignments are restricted to 3<sup>±</sup> or 4<sup>±</sup>. Since the 1163.03-keV transition, which feeds a 3<sup>-</sup> level, has a  $K$  conversion coefficient that excludes  $E1$  multipolarity, the 3<sup>-</sup> character of the 3644.94-keV level is established.

#### S. 3686.74-keV Level – 3<sup>±</sup>, 4<sup>±</sup>

The 2610.11-keV  $\gamma$  ray is observed to be in coincidence only with the 1076.63-keV  $\gamma$  ray (see Fig. 11 and Table V). This fact indicates an excited level at (1076.63  $\pm$  0.10) + (2610.11  $\pm$  0.20) = 3686.74  $\pm$  0.23 keV.

With a  $\log ft$  value of 6.9, the electron capture to this level is either allowed or first-forbidden, nonunique, with spin-parity choices of (3, 4, 5)<sup>±</sup> implied. Since the only transition (and it is a strong one) by which this state decays is to a 2<sup>+</sup> state, 5<sup>±</sup> and 4<sup>-</sup> are excluded.

#### T. 3765.59 $\pm$ 0.11-keV Level – (4, 5)<sup>-</sup>

This level is proposed to account for the following coincidence relationships: the 580.57-keV  $\gamma$  ray coincident with the 307.00-, 703.33-, 627.72-, 777.37-, 1854.38-, 1076.63-, 1024.04-, and 1801.70-keV  $\gamma$  rays (see Figs. 11, 13, 14, and 17–20 and Table V); the 709.90-keV line coincident with 382.86-, 443.13-, 826.02-, 1076.63-, and 1153.05-keV  $\gamma$  rays (see Fig. 22 and Table V); and the 1092.68-keV line coincident with 1076.63-, 1153.05-, and 443.13-keV  $\gamma$  rays (see Figs. 11, 15, and 16 and Table V). A line at 768 keV was observed to be in coincidence with the 1920.72-keV  $\gamma$  rays (see Fig. 12), but the previously placed 767.63-keV transition could account for neither the observation nor the intensity of this line in Fig. 12. Hence, it had to be assumed that the 768-keV line consists of two  $\gamma$  rays with the following energies calculated from the level energies and with intensities (in parentheses) deduced from the coincidence spectra:

$$767.63 \pm 0.13 \text{ keV } (2.9 \pm 0.4),$$

$$768.25 \pm 0.16 \text{ keV } (0.39 \pm 0.13).$$

The placement of these transitions leads to good energy sum relationships (in keV) of:

$$\begin{aligned}(3185.19 \pm 0.10) + (580.57 \pm 0.10) &= 3765.76 \pm 0.14, \\ (3055.66 \pm 0.17) + (709.90 \pm 0.10) &= 3765.56 \pm 0.19, \\ (2672.76 \pm 0.13) + (1092.68 \pm 0.13) &= 3765.44 \pm 0.18.\end{aligned}$$

The level energy was determined from a weighted average of these values.

By establishing the level at 3765.59 keV, one can place five additional  $\gamma$  rays ( $1535.67 \pm 0.13$ ,  $1283.96 \pm 0.13$ ,  $887.40 \pm 0.17$ ,  $448.1 \pm 0.5$ , and  $209.80 \pm 0.23$  keV) as transitions to already existing levels on the basis of energy sum relationships and some marginal coincidence evidence. The energy sum relationships in keV for these five lines are:

$$\begin{aligned}(2229.68 \pm 0.14) + (1535.67 \pm 0.13) &= 3765.35 \pm 0.19, \\ (2481.91 \pm 0.10) + (1283.96 \pm 0.13) &= 3765.87 \pm 0.16, \\ (2878.28 \pm 0.10) + (887.40 \pm 0.17) &= 3765.68 \pm 0.20, \\ (3317.58 \pm 0.20) + (448.1 \pm 0.5) &= 3765.68 \pm 0.70, \\ (3555.66 \pm 0.25) + (209.8 \pm 0.2) &= 3765.46 \pm 0.32.\end{aligned}$$

Since the 580.57- and 709.90-keV  $\gamma$  rays are  $M1/E2$ , the parity of this state is negative. The definite  $M1$  component in the 580.57-keV transition restricts the spins to 2–5. The low  $\log ft$  value of 6.0 for decay to this level is consistent with the negative parity and allowed decay, and limits the spin to 3–5. Absence of transitions to the  $2^+$  levels favors spin values 4 and 5.

#### U. 3774.80 $\pm$ 0.19-keV Level – $3^{\pm}, 4^{\pm}, 5^{\pm}$

There is coincidence evidence for the 1102.02-keV transition only in the 443-keV-gate spectrum. The 719.17 transition can also be placed from this level. The energy sum relationships (in keV) are:

$$\begin{aligned}(2672.76 \pm 0.13) + (1102.02 \pm 0.23) &= 3774.78 \pm 0.26, \\ (3055.66 \pm 0.17) + (719.17 \pm 0.23) &= 3774.83 \pm 0.28.\end{aligned}$$

The average of these two energies is the adopted level value.

The  $\beta$ -decay  $\log ft$  value of 7.3 indicates either allowed or first-forbidden nonunique transitions, and consequently, spins and parities of  $3^{\pm}, 4^{\pm}, 5^{\pm}$  are allowed.

#### V. 3831.06-keV Level – $(4, 5)^{-}$

This level has already been discussed in Sec. VII N.

#### W. 3871.53 $\pm$ 0.40-keV Level – $3^{\pm}, 4^{\pm}$

The 2794.90  $\pm$  0.35-keV  $\gamma$  ray is strongly in coincidence with the 1076.63-keV transition, which implies a level at  $(1076.63 \pm 0.10) + (2794.9 \pm 0.40) = 3871.53 \pm 0.37$  keV. Although not shown, this coin-

cidence relation is seen more clearly in the NaI (1076-keV gate)-Ge(Li) spectrum than in Fig. 11. The weak  $\gamma$  ray of 2017.11 keV can then be placed between the 3871.53- and 1854.20-keV levels because of energy considerations.

The  $\log ft$  value of 7.2 for the positron transition to the 3871.53-keV level is compatible with an allowed or first-forbidden nonunique feeding. The fact that the level decays to the first and second excited  $2^+$  levels restricts the spin and parity to  $3^{\pm}, 4^{\pm}$ .

#### X. 3925.89 $\pm$ 0.10-keV Level – $3^{\pm}, 4^{\pm}, 5^{\pm}$

This level is introduced to explain the following coincidence results:

- (1) The 1696.25-keV  $\gamma$  ray is found to be in coincidence only with the 1153.05- and 1076.63-keV transitions (see Figs. 15 and 11 and Table V).
  - (2) The 1253.11-keV line is observed to be in coincidence with the 443.13-, 1153.05-, and 1076.63-keV transitions (see Figs. 16, 15, and 11 and Table V).
  - (3) The 740.81-keV  $\gamma$  ray is coincident with the 307.00-, 703.33-, 627.72-, 1854.38-, 777.37-, and 1076.63-keV transitions (see Figs. 19, 11, 20, 13, and 14 and Table V).
  - (4) The 608.29-keV  $\gamma$  ray is coincident with the 835.67-, 627.72-, 777.37-, 1854.38-, and 1076.63-keV transitions (see Figs. 11, 23, and 14 and Table V).
  - (5) The coincidence data and energy fits are consistent with the placement of the 634.78-, 425.97-, and 370.28-keV  $\gamma$  rays as transitions to the 3291.08-, 3499.84-, and 3555.66-keV levels, respectively.
- There is excellent agreement among the energy sums (in keV) for this level:

$$\begin{aligned}(2229.68 \pm 0.14) + (1696.25 \pm 0.13) &= 3925.93 \pm 0.19, \\ (2672.76 \pm 0.13) + (1253.11 \pm 0.10) &= 3925.87 \pm 0.16, \\ (3185.19 \pm 0.10) + (740.81 \pm 0.13) &= 3926.00 \pm 0.16, \\ (3291.08 \pm 0.17) + (634.78 \pm 0.2) &= 3925.86 \pm 0.26, \\ (3317.58 \pm 0.20) + (608.29 \pm 0.10) &= 3925.87 \pm 0.22, \\ (3499.84 \pm 0.16) + (425.97 \pm 0.23) &= 3925.81 \pm 0.28, \\ (3555.66 \pm 0.25) + (370.28 \pm 0.17) &= 3925.94 \pm 0.30.\end{aligned}$$

A level energy of 3925.89 keV is calculated from a weighted average of the above values. Since the 1253.11-keV transition has  $E1$  multipolarity, the parity of the level is positive. The  $\log ft$  value of 6.0 for the  $\beta$  decay and positive parity indicates a first-forbidden nonunique transition, which restricts the spin to 3, 4, 5.

**Y. 3942.41 ± 0.22-keV Level – 3<sup>±</sup>, 4<sup>+</sup>**

In Fig. 11 the 2865.9-keV  $\gamma$  ray is seen to be weakly in coincidence with the 1076.63-keV line. This coincidence relation was seen more clearly in the NaI (gate)-Ge(Li) coincidence data. Furthermore, the 2088.09-keV line is in coincidence with the 777.37-keV  $\gamma$  ray. Introduction of a level at 3942.41 keV accounts for these coincidence relationships, which yield the following energy sums (in keV):

$$(1076.63 \pm 0.10) + (2865.90 \pm 0.33) = 3942.53 \pm 0.34,$$

$$(1854.20 \pm 0.10) + (2088.09 \pm 0.25) = 3942.29 \pm 0.27,$$

and an average level energy of 3942.41 ± 0.22 keV. The very weak 256.38-keV  $\gamma$  ray is placed between the 3942.41- and 3686.74-keV levels.

The measured  $\log ft$  value of 7.3 indicates that the electron capture to the 3942.41-keV level is allowed or first-forbidden nonunique, and further indicates spin-parity possibilities of 3<sup>±</sup>, 4<sup>±</sup>, 5<sup>±</sup>. Since the two strongest transitions from this level occur to the 2<sup>+</sup> states, the spin and parity are restricted to 3<sup>±</sup>, 4<sup>+</sup>.

**Z. 3968.84 ± 0.14-keV Level – 3<sup>±</sup>, 4<sup>±</sup>, 5<sup>±</sup>**

In the coincidence spectra obtained by gates set on the 1153.05- and 443.13-keV transitions (see Figs. 15 and 16), a 1296.03-keV  $\gamma$  ray is observed. These coincidence results are the principal arguments for establishing this level.

This level makes it possible to place 971.43-, 783.56-, and 469.24-keV  $\gamma$  rays as transitions to the levels at 2997.34, 3185.19, and 3499.84 keV, respectively. The following energy sums are obtained (in keV):

$$(2672.76 \pm 0.13) + (1296.03 \pm 0.23) = 3968.79 \pm 0.27,$$

$$(2997.34 \pm 0.11) + (971.43 \pm 0.18) = 3968.77 \pm 0.21,$$

$$(3185.19 \pm 0.10) + (783.56 \pm 0.26) = 3968.75 \pm 0.28,$$

$$(3499.84 \pm 0.16) + (469.24 \pm 0.25) = 3969.08 \pm 0.30.$$

The mean value of the four energy sums is 3968.84 ± 0.14 keV. Spin-parity assignments of 3<sup>±</sup>, 4<sup>±</sup>, 5<sup>±</sup> are possible, as the  $\log ft$  value of 6.7 for the positron branch to the 3968.84-keV level indicates an allowed or first-forbidden nonunique transition.

**AA. 4146.0 ± 0.4-keV Level – 3<sup>±</sup>, 4<sup>+</sup>**

This level is required to explain the observation of a coincidence peak at 3069.7 keV in the coincidence spectrum obtained with the gate set on the 1076.63-keV line (see Fig. 9). The weak peak shown as 3040 keV in this figure has an uncertainty of 30 keV. This level can be used to place the 2291.8- and 380.4-keV  $\gamma$  rays, for which no coinci-

dence information is available. The level energy was taken as the weighted average of the following energy sums (in keV):

$$(1076.63 \pm 0.10) + (3069.7 \pm 0.4) = 4146.3 \pm 0.4,$$

$$(1854.05 \pm 0.10) + (2291.8 \pm 0.5) = 4145.8 \pm 0.5,$$

$$(3765.59 \pm 0.11) + (380.4 \pm 0.9) = 4146.0 \pm 0.9.$$

A  $\log ft$  value of 6.9 for the  $\beta$  decay limits the spin-parity to (3, 4, 5)<sup>±</sup>. Since strong transitions occur to the low-lying 2<sup>+</sup> states, these are further restricted to 3<sup>±</sup>, 4<sup>+</sup>.

**BB. 4206.00 ± 0.12-keV Level – 3<sup>±</sup>, 4<sup>±</sup>, 5<sup>-</sup>**

Coincidence spectra taken with gate settings on the 627.72-, 777.37-, 1854.38-, and 1076.63-keV lines show a strong peak at 1724.15-keV  $\gamma$  ray (see Figs. 11, 13, and 15 and Table V). These results are explained by proposing a level at 4206.00 keV. In addition, several other weak lines can now be placed into the decay scheme. The 1533.19- and 1327.5-keV  $\gamma$  rays are assumed to occur between the 4206.00-keV level and the 2676.76- and 2878.28-keV levels, respectively. Energy sums which define the level are (in keV):

$$(2481.91 \pm 0.10) + (1724.15 \pm 0.10) = 4206.06 \pm 0.14,$$

$$(2672.76 \pm 0.13) + (1533.19 \pm 0.13) = 4205.95 \pm 0.17,$$

$$(2878.28 \pm 0.10) + (1327.5 \pm 0.5) = 4205.8 \pm 0.5.$$

An adopted energy for this level is obtained from a weighted average of the more accurate first two sums.

Although not shown here, the coincidence spectra obtained by gating on the 382.86- and 826.02-keV transitions exhibited a peak at 1153 keV with a width about twice that expected. Further, there appears to be a photopeak at approximately 1150 keV in the coincidence spectrum obtained by gating on the 1153.05-keV  $\gamma$  ray. These results lead to the placement of a 1150.34-keV  $\gamma$  ray between the 4206.00- and 3055.66-keV levels.

From the  $\log ft$  value of 6.7 for the  $\beta$  decay (allowed or first-forbidden nonunique) and from the observation of a transition to a 3<sup>-</sup> state, the allowed spin-parity assignments are 3<sup>±</sup>, 4<sup>±</sup>, 5<sup>-</sup>.

**CC. 4339 ± 1.5-keV Level**

This level is proposed to explain the 1154-keV transition observed in coincidence with gates set on the 627.72- and 703.33-keV  $\gamma$  rays (see Table V and Figs. 14 and 20).

**DD. 4410.5 ± 0.7-keV Level – 3<sup>±</sup>, 4<sup>+</sup>**

A level at 4410.5 keV is required to explain the presence of the 3334.0-keV  $\gamma$  ray in the 1076.63-

keV gate (see Fig. 9 and Table V) and its absence in the 1854-keV NaI gate. In addition,  $\gamma$  rays of 2555.3 and 2180.8 keV are placed from this level to the levels at 1854.20 and 2229.68 keV, respectively. The following energy sums (in keV) can then be obtained:

$$(1854.20 \pm 0.10) + (2555.3 \pm 1.7) = 4409.5 \pm 1.7,$$

$$(2229.68 \pm 0.14) + (2180.8 \pm 1.0) = 4410.5 \pm 1.0,$$

$$(1076.63 \pm 0.10) + (3334.0 \pm 0.5) = 4410.6 \pm 0.5.$$

A weighted average of these sums is adopted as the energy of the level, viz., 4410.5 keV.

Spin-parity assignments of  $3^+$ ,  $4^+$ ,  $5^+$  are allowed by the  $\log ft$  value of 7.2 for the  $\beta$  decay. Transitions to the low-lying  $2^+$  states restrict this selection to  $3^+$ ,  $4^+$ .

#### EE. 4718 $\pm$ 2-keV Level - $3^+$ , $4^+$

Observation of a 3642-keV  $\gamma$  ray in the spectrum in coincidence with the 1076.63-keV gate (see Fig. 9) provides the primary evidence for a level at 4718 keV. The 3630-keV photopeak in this figure has an uncertainty of 15 keV. A second  $\gamma$  ray of 2862 keV is placed as the transition from this level to the 1854.20-keV level. The energy adopted for this level is a weighted average of the two energy sum relationships.

The  $\log ft$  value of 6.4 for the  $\beta$  decay and the decay characteristics of this level to the low-lying  $2^+$  levels indicate that the spin and parity of this state is  $3^+$ ,  $4^+$ .

#### FF. 4954 $\pm$ 6-keV Level - $3^+$ , $4^+$

A level at 4954 keV is required to explain the presence of a  $\gamma$  ray of about 3877 keV in the 1076.63-keV gate (see Fig. 9). The  $\log ft$  value of 6.8 for the  $\beta$  decay and the decay of this level to the first  $2^+$  level indicates that the spin and parity of this state is  $3^+$ ,  $4^+$ .

### VIII. DISCUSSION

The  $^{86}\text{Sr}$  nucleus consists of 38 protons which fill the  $1f_{5/2}$  and lower-lying subshells and of 48 neutrons which have two holes in the  $1g_{9/2}$  subshell. Talmi and Unna<sup>2</sup> have calculated excited states in  $^{86}\text{Sr}$  under the assumption that the closed  $1f_{5/2}$  subshell is stable as far as the low-lying levels are concerned; they only considered the neutron holes in the  $2p_{1/2}$  and  $1g_{9/2}$  subshells. Their calculations predict excited states at 1.08 ( $2^+$ ), 1.98 ( $4^+$ ), 2.33

( $0^+$ ), 2.35 ( $6^+$ ), 2.49 ( $8^+$ ), 2.58 ( $5^-$ ), and 2.62 ( $4^-$ ) MeV. The agreement with the experimental level scheme is not very good. One reason for this may be that proton excitations also occur and account for some of the higher-lying states. This seems to be the case for  $^{88}\text{Sr}$ , which has 50 neutrons that form a very stable closed shell, and as a consequence only protons of the closed  $1f_{5/2}$  subshell can be excited at low energies. The  $^{88}\text{Sr}$  nucleus shows an excited  $2^+$  level at 1.84 MeV and a  $3^-$  level at 2.74 MeV.

It appears from the experimental level scheme of  $^{86}\text{Sr}$  that the 2997.34-keV  $3^-$  level decays preferentially to the 1076.63-keV  $2^+$  level, whereas the 2481.91-keV  $3^-$  level feeds principally the 1854.20-keV  $2^+$  level. Thus, it seems reasonable to assume that the 1076.63-keV  $2^+$  and 2997.34-keV  $3^-$  levels are due to neutron configurations and that the 1854.20-keV  $2^+$  and 2481.91-keV  $3^-$  levels arise from proton excitations, as proposed earlier.<sup>13</sup>

Collective effects also are probably very important in the  $^{86}\text{Sr}$  level structure. The 1076.63-keV  $2^+$  level may be described as a one-phonon vibrational level, whereas the 1854.2-keV  $2^+$  level may be described as a member of the two-phonon triplet, and the 2229.68-keV level could be the  $4^+$  member. Computing the ratio of reduced  $E2$  transition probabilities of the 777.37-keV stopover to the 1854.20-keV crossover transitions, one obtains  $B(E2; 2_2^+ \rightarrow 2_1^+)/B(E2; 2_2^+ \rightarrow 0_1^+) \approx 102$ , where it is assumed that the 777.37-keV line is pure  $E2$ . The 2481.91-keV  $3^-$  level may be interpreted as the one-phonon octupole level because of a relatively strong transition to the ground state. It is not possible to make any predictions about the higher excited states until unique spin assignments become possible.

### IX. ACKNOWLEDGMENTS

The authors would like to acknowledge the help of Mrs. Susan Keith, Mrs. Lynda Kern, and Allen Joseph during the various stages of data processing, and are grateful to A. P. Callahan for his assistance in processing the targets. Final typing of the manuscript by Mrs. Susan Keith is appreciated very much. Our thanks are extended to Dr. Hultberg and his collaborators for the calculation of the  $f_K$  factors. Dr. A. V. Ramayya and Dr. J. H. Hamilton would like to thank Oak Ridge Associated Universities for their fine cooperation in terms of a travel grant.

\*Present address: Technological University of Delft, Department of Physics, Delft, The Netherlands. Part of this work was performed while this author was on a

National Science Foundation Senior Foreign Scientist Fellowship.

†Present address: Boris Kidric Institute of Nuclear

Science, Belgrade, Yugoslavia.

‡Work supported in part by a grant from the National Science Foundation.

§Research sponsored by the U. S. Atomic Energy Commission under contract with Union Carbide Corporation.

<sup>1</sup>A. Bohr and B. R. Mottelson, *Kgl. Danske Videnskab. Selskab, Mat.-Fys. Medd.* **27**, No. 16 (1953).

<sup>2</sup>I. Talmi and I. Unna, *Nucl. Phys.* **19**, 225 (1960).

<sup>3</sup>T. Yamazaki, H. Ikegami, and M. Sakai, *Nucl. Phys.* **30**, 68 (1962).

<sup>4</sup>B. Van Nooijen, W. Lourens, H. Van Krugten, and A. H. Wapstra, *Nucl. Phys.* **63**, 241 (1965).

<sup>5</sup>A. C. Rester, Ph. D. thesis, Vanderbilt University, 1969 (unpublished).

<sup>6</sup>Q. L. Baird, J. C. Nall, S. K. Haynes, and J. H. Hamilton, *Nucl. Instr. Methods* **16**, 275 (1962).

<sup>7</sup>R. H. Pratt, R. D. Lever, R. L. Pexton, and W. Aron, *Phys. Rev.* **134**, A898 (1964).

<sup>8</sup>R. S. Hager and E. C. Seltzer, *Nucl. Data* **A4**, 1 (1968).

<sup>9</sup>C. M. Lederer, J. M. Hollander, and I. Perlman, *Table of Isotopes* (John Wiley & Sons, Inc., New York, 1967), 6th ed.

<sup>10</sup>A. V. Ramayya, J. H. Hamilton, J. A. Deye, R. L. Robinson, and J. L. C. Ford, private communication.

<sup>11</sup>*Nuclear Data Sheets*, compiled by K. Way *et al.* (Printing and Publishing Office, National Academy of Sciences - National Research Council, Washington, D. C.).

<sup>12</sup>R. G. Arns, D. V. Martin, W. G. Monahan, and S. W. Sprague, to be published.

<sup>13</sup>A. V. Ramayya, J. H. Hamilton, J. A. Deye, R. L. Robinson, and J. J. Pinajian, *Nucl. Phys.* **A127**, 60 (1969).

PHYSICAL REVIEW C

VOLUME 2, NUMBER 6

DECEMBER 1970

## Lifetimes of Excited Levels and Electromagnetic Transition Rates in <sup>51</sup>V, <sup>75</sup>As, <sup>90</sup>Y, and <sup>123</sup>Sb

H. Singh, B. Sethi, and S. K. Mukherjee

*Saha Institute of Nuclear Physics, Calcutta-9, India*

(Received 7 April 1970; revised manuscript received 13 July 1970)

The lifetimes of the excited states in <sup>51</sup>V, <sup>75</sup>As, <sup>90</sup>Y, and <sup>123</sup>Sb have been measured by the delayed-coincidence technique using a time-to-amplitude converter. The results are  $T_{1/2}(319.5 \text{ keV}, ^{51}\text{V}) = 0.190 \pm 0.030 \text{ nsec}$ ,  $T_{1/2}(927.5 \text{ keV}, ^{51}\text{V}) = 0.070 \pm 0.025 \text{ nsec}$ ,  $T_{1/2}(198.0 \text{ keV}, ^{75}\text{As}) = 0.75 \pm 0.15 \text{ nsec}$ ,  $T_{1/2}(202.7 \text{ keV}, ^{90}\text{Y}) = 0.180 \pm 0.030 \text{ nsec}$ ,  $T_{1/2}(160.2 \text{ keV}, ^{123}\text{Sb}) = 0.60 \pm 0.08 \text{ nsec}$ . The energies and relative intensities of the  $\gamma$  rays in these nuclei have been determined with the help of a Ge(Li) detector. On the basis of these measurements and the values of multipole mixing ratios, the reduced  $B(M1)$  and  $B(E2)$  transition probabilities have been deduced for various transitions in these nuclei. The hindrance and enhancement factors are determined with respect to the Weisskopf single-particle estimates for  $M1$  and  $E2$  transitions, respectively.

### INTRODUCTION

In the present investigation we have measured the lifetimes of the excited states in <sup>51</sup>V, <sup>75</sup>As, <sup>90</sup>Y, and <sup>123</sup>Sb using the delayed-coincidence technique. The measurements of the half-lives of the 927.5- and the 202.7-keV levels in <sup>51</sup>V and <sup>90</sup>Y, respectively, are being reported for the first time. In the case of the 198.0-keV level in <sup>75</sup>As, only one report is available,<sup>1</sup> giving a half-life of 0.9 nsec using the pulsed-beam technique. The measurements of the half-lives in the case of the 319.5-keV level in <sup>51</sup>V and 160.2-keV level in <sup>123</sup>Sb have been repeated in the present work as check experiments.

Also we have measured the energies, intensities, and branching ratios of the  $\gamma$  rays in these nuclei with a Ge(Li) detector. This new information together with the earlier known electron intensities, total conversion coefficients, and multipole mix-

ing ratios, has made it possible to deduce reduced  $B(M1)$  and  $B(E2)$  transition probabilities from our measured lifetimes.

### EXPERIMENTAL PROCEDURE

The lifetimes were measured with the help of a fast-slow coincidence set up using a time-to-amplitude converter (ORTEC model No. 263) and a 512-channel analyzer (ND 120). For the detection of  $\beta$  and  $\gamma$  rays, detectors consisting of 2.5-cm-diam  $\times$  3-mm-thick NE810 and 2.5-cm-diam  $\times$  2.5-cm-long NE102A plastic scintillators, respectively, optically coupled to RCA 7850 photomultipliers, were used. The time resolution [full width at half maximum (FWHM)] of the whole system was 0.6 nsec, and the slope (= instrumental half-life) was 0.14 nsec as measured with a <sup>60</sup>Co source. Details of the electronic system and time calibration have been given previously.<sup>2</sup>